Formability Analysis of Polymers in Incremental Sheet Forming Process

Aminreza Mahna

Submitted to the
Institute of Graduate Studies and Research
in partial fulfilment of the requirements for the Degree of

Master of Science
in
Mechanical Engineering

Eastern Mediterranean University
August 2013
Gazimağusa, North Cyprus

Approval of the Institute of Graduate Studies and Research

Prof. Dr. Elvan Yılmaz
Director

I certify that this thesis satisfies the requirements as a thesis for the degree of Master of Science in Mechanical Engineering.

Assoc. Prof. Dr. Uğur Atikol
Chair, Department of Mechanical Engineering

We certify that we have read this thesis and that in our opinion it is fully adequate in scope and quality as a thesis for the degree of Master of Science in Mechanical Engineering.

Assist. Prof. Dr. Ghulam Hussain
Supervisor

Examining Committee

1. Prof. Dr. Majid Hashemipour

2. Assist. Prof. Dr. Ghulam Hussain

3. Assist. Prof. Dr. Neriman Özada

ABSTRACT

Single point incremental forming (SPIF) being simple and flexible has potential to replace conventional process in order to produce customized cost-effective parts. It has found several applications in automobile, aerospace and biomedical industries. Traditional processing of polymers normally requires dedicated tools, long setup times and high investments. Therefore, there is a need to find an economical alternative of traditional processing. In this study, the ability of SPIF to process polymers is examined at room temperature. Two polymer materials, polyvinylchloride (PVC) and polyethylene (PE) are employed. The said objective is done through examining the formability of these polymer sheets by varying process parameters, namely tool radius, spindle rotation and step size. To do so, a frustum of cone with wall angle continuously varying along depth is used as test geometry. The formability is defined in two ways: maximum wall angle corresponding to commencement of wrinkling and maximum wall angle corresponding to fracture point. To examine the effect of temperature, if any, on sheet failure during SPIF, temperature rise is recorded in each test. The test plan following response surface method is prepared using a statistical package, Design Expert Dx-8.

The tests results have shown that the formability of PVC is limited by sheet fracturing and the formability of PE is limited by sheet wrinkling. Moreover, the combination of parameters, instead of an individual one, is more meaningful to control formability in SPIF. Further, high-high combination (i.e., high values of parameters) is useful for improving formability of PVC, whereas low-low combination of parameters is useful to enhance formability of PE. Temperature rise

during SPIF has been found to be the major reason behind the above findings, which have been detailed in the thesis. Finally, to predict the formability for both of PVC and PE material, empirical models as function of process parameter have been proposed.

Keywords: Single point incremental forming, polymers, PVC, PE, formability, maximum wall angle, fracture, wrinkling.

ÖZ

Tek nokta artan şekillendirme (SPIF) basit ve esnek olan özelleştirilmiş maliyetli parçaları üretmek için kullanılan bir uygulamadır. Bu şekillendirme havacılık, otomotiv ve biyomedikal gibi çeşitli uygulama alanlarında kullanılmaktadır. Polimerlerin Geleneksel işlemesi normalde uzun kurulum süresi ve yüksek yatırımlar gerektirir. Bu nedenle, geleneksel bir işlem ve ekonomik bir alternatif bulmak ihtiyaç haline gelmiştir. Bu çalışmada, proses polimerlerin SPIF kabiliyeti oda sıcaklığında incelenir. İki polimer malzeme olan polivinilklorür (PVC) ve polietilen (PE) kullanılır. Amaç, parametreleri, takım yarıçapı, iş mili dönüşünü ve adım boyutu değişen bu polimer levhaların şekillendirilebilirliğinin incelenmesidir. Bunu kesik koni testi olarak kullanılır.Şekillendirilebilirlik iki şekilde tanımlanır: kırışıklıklar ve nokta kırılmaya karşılık gelen maksimum duvar açısı. SPIF sırasında levha sıcaklığının etkisi, eğer varsa, sıcaklık artışı, her bir testte kaydedilir. Bu tezde bir istatistik paket olan Tasarım Uzmanı Dx-8 kullanılmıştır.

Test sonuçları PVC'nin şekillendirilmesinin levha kırılması ile sınırlı olduğunu ve PE'nin şekillendirilmesinin de levha kırışma ile sınırlandırılmış olduğunu göstermiştir. Ayrıca, bunun yerine, parametrelerin oluşturduğu kombinasyon, SPIF bölgesindeki şekillendirilebilirliği kontrol etmek için daha uygundur. Parametrelerinin düşük-düşük kombinasyonu PE ile şekillendirilebilirliğin artması için yararlı ise, PVC'de şekillendirilebilirliğin iyileştirilmesi için yararlıdır. SPIF sırasında sıcaklık artışının bulguların arkasındaki en önemli neden olduğu tespit edilmiştir. Son olarak, PVC ve PE malzemelerinin her ikisi için de

şekillendirilebilirliliği tahmin etmek için, işlem parametresinin fonksiyonu deneysel model olarak önerilmiştir.

Anahtar Kelimeler: Tek noktadan artan şekillendirme, polimerler, PVC, PE şekillendirilebilirlik, maksimum duvar açısı, kırık, kırışıklıklar.

ACKNOWLEDGMENTS

First, I would like to express my thankfulness to my supervisor, Assist. Prof. Dr.Ghulam Hussain for his invaluable scientific advice, discussions and suggestions that provided a stimulating guidance throughout this work. The Department Chair Assoc. Prof. Dr.Ugur Atikol and all the lecturers and assistances of the department. I also would like to thank the mechanical department work shop staffs for their honesty and help in manufacturing required equipment's. I want to express my special gratitude Atieh for her encouragement and support. Finally, I would like to address my acknowledgements to my parents for their unlimited love and supports during my whole life specially my Education.

.

TABLE OF CONTENTS

LIST OF TABLES

LIST OF FIGURES

IF Incremental forming

ISF Incremental Sheet forming

SPIF Single Point Incremental Forming

TPIF Two Point Incremental Forming

NIF Negative Incremental Forming

PE Polyethylene

PVC polyvinylchloride

NC Numerical Control

FEA Fainant Element Analysis

DOE Design OF Experiments

CNC Computer Numerical Control

CAD Computer Aided Design

CAM Computer Aided Manufacturing

ASTM American Society for Testing and Materials

3D Three Dimensional

HSS High Speed Steel

HRC Rockwell Hardness

ANOVA Analysis Of Variance

RS Response Surface

Chapter 1

INTRODUCTION

In most of the manufacturing industries, sheet metal forming is one of the main production processes. Throughout the decades, technological advances have accepted challenges to manufacture intricate parts. To repay the costs of dies and tooling, the economic competitiveness of the process needs large production batches. Therefore, small and medium volume production using conventional processes such as deep drawing and stamping has been a problem of the metalworking industry. On the other hand, the customer's requirements are changing, according to which they demand for specialized and customized products. To meet such demands, the industrialized companies have to get used to a new surroundings which requires more flexible operations to satisfy different market segments. As a result, invention of sheet forming processes with shorter production cycles is necessitated in order to reduce development time of products [1, 4].

To fulfill the above-said objective, several methods characterized by high flexibility were introduced, e.g. water jet forming, laser forming and NC incremental forming. Owing to high simplicity and low-cost tooling, incremental sheet forming (ISF) has attained the greatest attention. It is capable to process both metal and non-metals. Further, it can shape intricate parts which are difficult to form with traditional processes, in a rapid and economic way without expensive dies and long set-up times [2].

1.1 Types of Incremental Forming Process

In fact, the incremental forming has long been practiced in past to form part, e.g., metal spinning [3]. However, it differs from the new incremental process. Due to this reason, incremental forming processes can be divided into two types:

1. Conventional incremental forming processes
2. Modern incremental forming process

1.1.1 Conventional Incremental Forming Processes

Incremental Sheet forming is getting start with spinning in Egypt, then it is developed and outfitted in china, afterwards it transferred to England and USA at beginning of the 20^{th} century. In that time expert and skillful labors are considered to perform some initial parts like cooking instruments on a Primary lathe machine. Growing of requests for modern manufacturing products, such as military, medical, airspace and automotive products, cause that spinning is going to be evaluated for new technology of incremental forming [4].

1. Spinning

An excellent means for swift prototyping round unfilled metal forms is spinning (see figure 1.1). A disc blank is clamped against a mandrel on a spinning lathe. The forming tool sweeps the blank to produce a copy of the mandrel and the mandrel is rotated at high revolutions. This action is occurred in a number of sweeps and it is controlled manually or automatically. Reducing of the diameter of the disc blank and unchanging wall thickness of spun part stands, lastly [8].

Only with one roller, conventional spinning is generally carried out. Nevertheless, two rollers are placed diametrically over each other in cases where thick sheet metals need to be spun, in order to balance the applied loading [2].

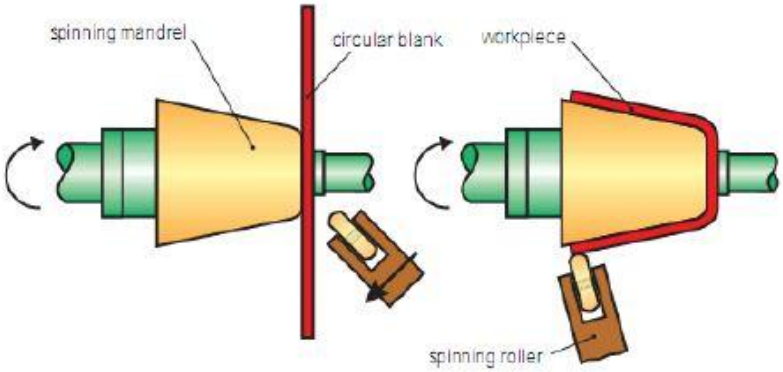

Figure1. 1: Spinning

2. Flow Forming

A process which shaped the product from metal blank in hollow or tube types is flow forming. One or more rollers are used to flow axially the material along the mandrel. Considerably, the thickness of the blank changed in flow forming is the basic distinction between the spinning and flow forming [5].

According to the direction of flow of material, it can be divided into two types: (a) forward flow forming, and (b) backward flow forming (see figure 1.2). Forward flow forming is usually employed for blanks with base or rings with internal flange. Between the tail stock and mandrel the blank is held. As that of the traversing roller, the roller forces the material to flow in the same direction. To manufacture high precision parts such as rocket motors this method is often employed. When blank does not have base such as sleeve or ring without internal flange Backward flow forming is worked. Against the tailstock the blank is held and the material is pushed onto the mandrel. Towards the unsupported mandrel's ending, the material is forced to flow in the opposite direction to the roller [6].

When the original ductility of the blank is too low to contain tensile stresses, such as cast and welded parts, backward flow forming is particularly appropriate. Producing components by backward method are more worthwhile than those produced by forward method. On the other hand, the forward method is not as industrious as backward method [5].

The final wall thickness of a cylindrical component produced by flow forming is governed by the following connection:

$$t = (D_o - D)/2 \qquad (1.1)$$

Where

The wall thickness of cylindrical component is t

The outer diameter of cylindrical component is D_o

The internal diameter of cylindrical component is D

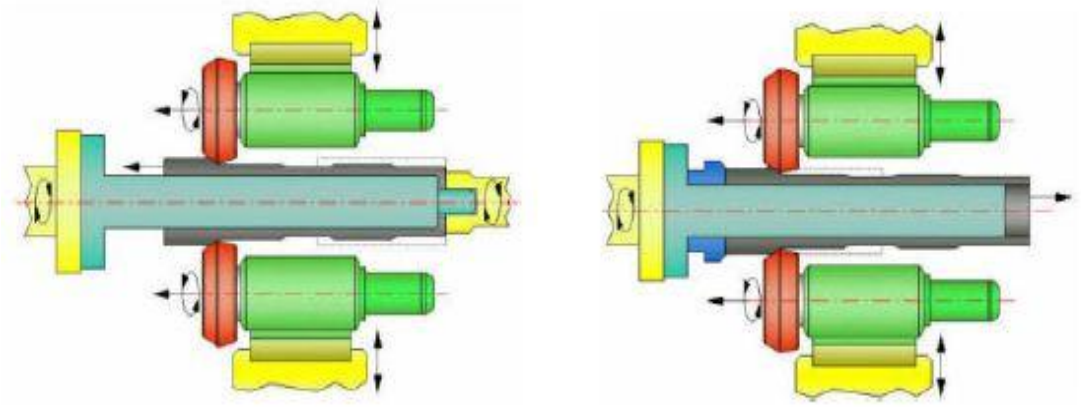

Figure1. 2: Backward and forward flow forming

3. Shear Forming

The fundamental of the previous spinning technology with the using of the hydraulic equipment and CNC technology is common as shear forming process. There is a

particular similarity between the machine which uses for shear forming and spinning forming. While, it is intended to able to situate a higher strength during shear forming process. The thickness of blank is less distorted than one in shear forming in the conventional spinning process. In general, the process is done in one pass, in contrast with conventional spinning [9]. Hence, no substantial deformation occurs along radial axis and the roller-shaped tool dislocates the material equivalent to the axis of mandrel (Figure.3). Furthermore, the projection remains vertical to the forming axis and the blank's outer diameter remains unmoved [5]. Consequently, the procedure is called as shear forming process (see figure 1.3). Following convention can be calculated the final thickness of a shear formed part:

$$t = t_o . sin\alpha \qquad (1.2)$$

Where

t_o Is equal to the initial thickness of Blank

α is equal to the half-apex angle of cone

t is equal to the final wall thickness

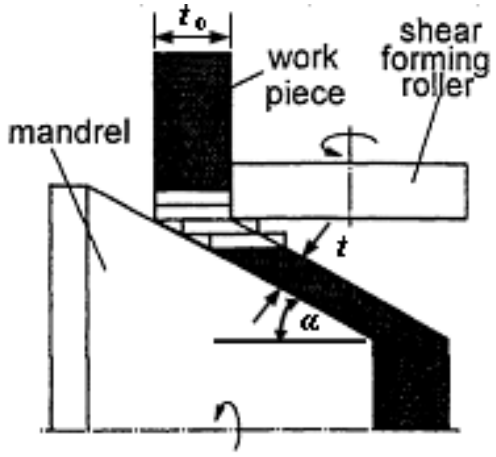

Figure1. 3: Shear forming

The above formula is known as sine law. The final wall thickness of components should go after the sine law, in order to avoid forming defects in shear forming.

Then, flange wrinkling is due to the wall thickness larger than sine law, and flange bending is because of the wall thickness smaller than sine law [10].

1.1.2 Modern Incremental Forming Process

To produce a part from the sheet materials, forming approach which uses the numerically controlled (NC) technology is called ISF technology. The original product can be made in one day from CAD modeling to ended part with this technology. The incremental sheet forming techniques (ISF) can be separated into two classes: Two points incremental forming (TPIF) and single point incremental forming (SPIF), also identified as negative and positive forming [14].

1. Two Point Incremental Forming (TPIF):

The sheet metal transfers vertically on bearings, which move on sheet holder posts, alongside the z-axis, as the forming tool pushes into the metal sheet in TPIF process (Figure1.4). This procedure is called TPIF because it has two contacting points between the sheet and forming tool. The first point is plastic deformation which occurs where forming tool presses down on the sheet metal locally. A contacting point between a static post and the sheet creating when the tool pushed into the sheet is the second point of this process. TPIF method used a fractional die, although it is often called as die less forming [10].

The TPIF process can be categorized into two sorts: TPIF with a static support (figure 1.4), and TPIF With a kinematic support (figure 1.5). In TPIF with a static support the support is located definitely on the opposite side of the sheet metal (opposite with contacting surface between tool and sheet). The sheet metal is fastened inflexibly on a surround that can go up and down in the similar direction of the tool[7].

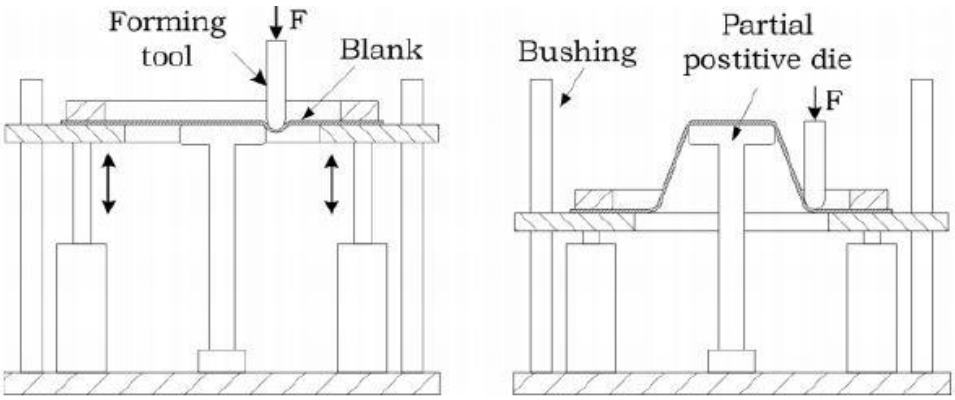

Figure1. 4 : Two Points Incremental Forming

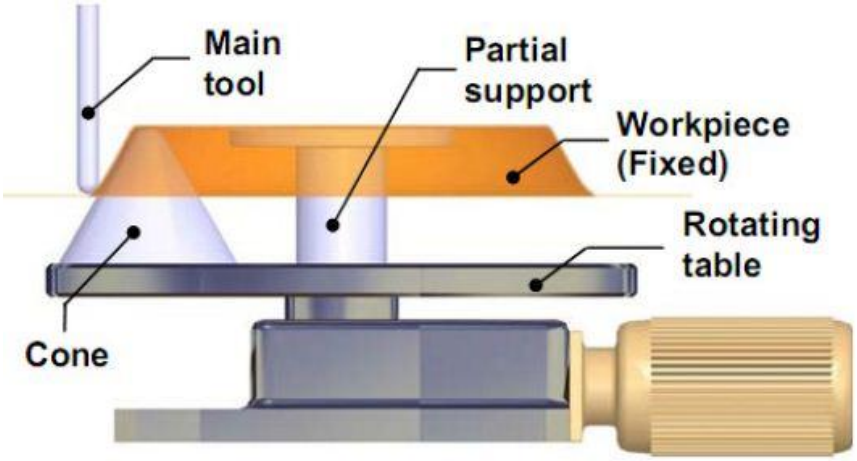

Figure1. 5: TPIF with kinematic support

As shown in Figure 1.5 In kinematic TPIF, the partial support is fixed on a rotating table which rotates concurrently with forming tool. The rotating table holds a patrial die that has a shape of final product. This system has the disadvantage to be only appropriate for rotational symmetry products [7].

2. Single Point Incremental Forming (SPIF)

In order to form complicated shapes by TPIF, a die of the same shape of constituent is needed. Although the use of die not costly, the flexibility of the process reduces. Jeswiet and several other scholars [2] improved the TPIF process with the intention of the goal achievement of high flexibility to prevent the use of dies. Single point

incremental forming (SPIF) or negative incremental forming (NIF) is named by researchers who abolished the use of dies by pressing sheet on single point, i.e. and deformation point in this process[13].

The machine in which uses in SPIF process is more simpler than TPIF process, that it does not requirement for bushings vertical motion of blank as shown in figure 1.6 . From the periphery to the center of blank the sheet is formed, contrary to TPIF. The deformation of sheet area is not supported; therefore, any complicated shape can be formed without die just by numerically controlling the tool motion. The SPIF process can be classified into two types: (1) single pass SPIF and (2) multi pass SPIF. In the former kind, the final product is formed in one pass, however in the latter kind; numerous passes are employed to formed a part. The wall thickness of a part in single pass SPIF follows the sine law similarly to shear forming [9]; consequently, vertical walls cannot be formed. In contrast, higher wall thickness than the sine law's prediction can be obtained in multi pass SPIF process, thus, producing components with vertical walls makes it possible to [11].

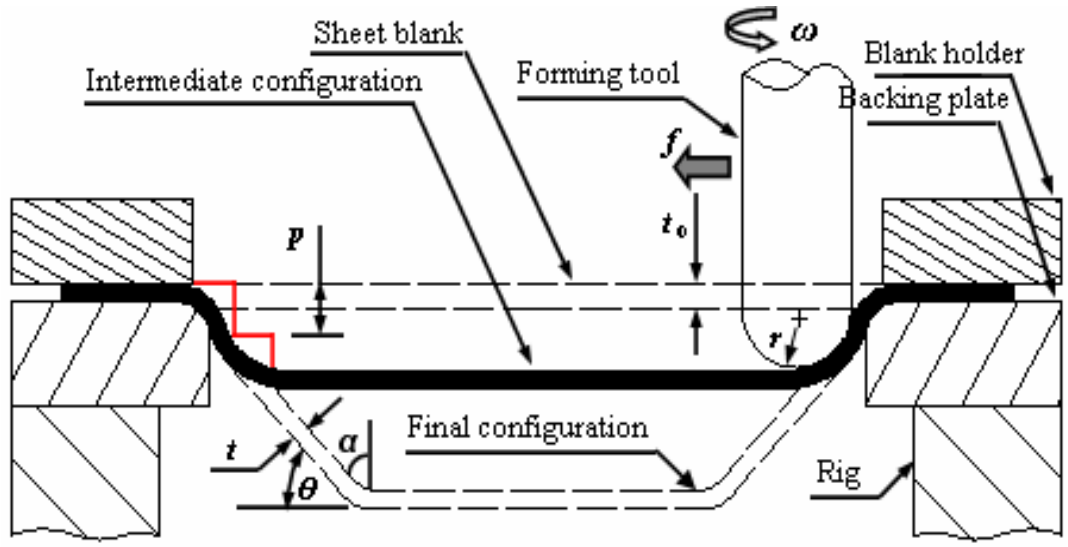

Figure1. 6: Single point incremental forming

1.2 Applications of New Incremental Forming Process

As a more cost proficient alternative to more current conventional sheet pressing processes, the process of incremental sheet forming has been perceived. The preference for low-volume, high value applications are supported by the ISF procedure [4]. Therefore, the ability to produce asymmetrical parts out of a large multiplicity of metals is greatly increased the field of application concerning ISF processes. Accounting the high flexibility with short set-up times can be the further preference to this method. The ISF method is applied in most manufacturing sectors (figure 1.7) that necessitate small to medium size batches as a supporter of various and unique designs due to the high flexibility. In contrast with conventional sheet metal stamping processes as studied by Jeswiet et al, the high end product forming flexibility in the ISF process is higher [2].

Figure1. 7: a) Reflexive surface for headlights & b) automotive heat/vibration shield

Biomedical Applications

For biomedical applications the IF process has been applied. The ISF method can be helpful for biomedical applications due to high degree of customized requirements (see figure 1.8) [16]. The application of IF techniques for the manufacturing of customized medical orthopedic products is revised by Ambrogio et al, which is focused on the sheet profiling of the producing a customized ankle support for a

patient. He discussed the same process which can be applied to several biomedical product advance applications [17].

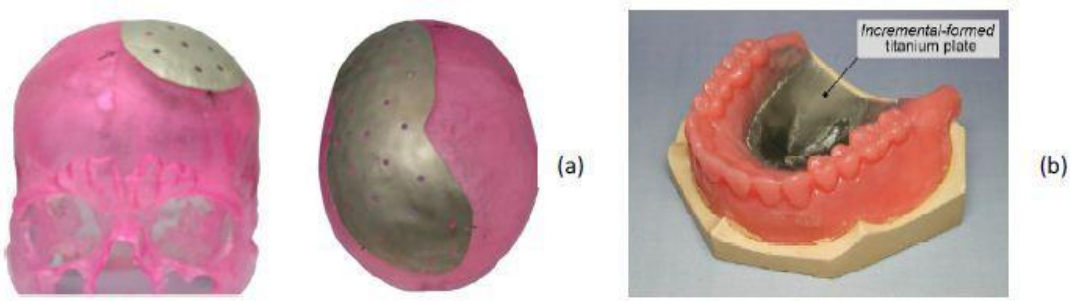

Figure1. 8: Biomedical applications

1.3 Formable Materials

There are various materials that can be formed by incremental forming process which are described in literature review [19]:

1. Aluminum alloys and other metal material
2. Sandwich panels
3. Polymer and composite
4. Magnesium
5. Titanium

1.4 Advantages of Single Point Incremental Forming (SPIF)

ISF potential advantage is no requirement for dedicated dies or exclusive forming tools. A desired part can be produced in a day; then, it is very suitable to small production batch or rapid prototype. In comparison with conventional forming another advantage is a high deformation level [14].

There are central advantages of the SPIF Process:

- To form the products the process does not require dies, removing the production costs otherwise used for custom dies.
- Using design software can be modified by designing parts which are considered as highly flexible as design sizes.
- One of the easiest rapid prototyping methods of metal products is the ISF process.
- Using conventional CNC milling machines, eliminating large mentioned costs can be performed by the process.
- As it only implicates a round tipped forming tool, the need for specialized tooling is minimized.
- The components produced from the CAD file directly;
- Changing designs can be rapidly and easily performed;
- Forces are small due to the incremental nature of the process;
- Parts' dimensions are only restricted by the machine tool;
- The final good surface quality can be obtained;

1.5 Shortcomings of ISF

ISF method required long operation time due to small deformations and when in compared to conventional forming process such as stamping it is find that conventional methods are slower than ISF [15]. A number of shortcomings of ISF process are listed as following.

- Longer forming time in contrast with conventional Processes;
- There is less geometry validity, especially in convex radii and bending edges parts [11]

- The process is limited to small batch sizes, with the intention of be economically viable [10]
- The forming of right angles cannot be performed in a single step for 3-axis CNC applications, nonetheless requires a multi-step process.
- If the implemented tool path designs do not recompense for this aspect, spring back can happen.

1.6 Polymers: Applications and Manufacturing Methods

Polymers play a very important role in manufacturing of parts. In recent decades, the application of polymers has been increased in many sectors of industry such as automotive parts, aerospace and biomedical components [22]. Moreover, with the using of polymers and composites, the substitution of light-parts instead of heavy segments is an approach to modern manufacturing industry. Detailed applications of these materials are given as follows:

1.5.1 Applications of Polymers

Polymer materials are ideally suited for industrial applications due to their e.g. light weight, ease of manufacture, flexibility in usage, good thermal and electrical insulation properties (see figure 1.9). Their applications can be exampled as following parts [31]:

Agriculture and Agribusiness

Polymers are being used in soil in order to improve aeration, promote plant growth, and mulch providing.

Medicine

Some biomaterials, such as blood vessels and heart valve replacements are made of polymers like polyurethane, Dacron and Teflon.

Consumer Science

Plastic containers of all sizes and shapes are light weight and economically less expensive than the more traditional containers. Clothing, floor coverings, and packaging are other polymer applications.

Industry

Automobile components, fighter planes windshields, pipes, tanks, packing materials, insulation, wood substitutes, adhesives, matrix for composites, and elastomers are all polymer applications used in the industrial market.

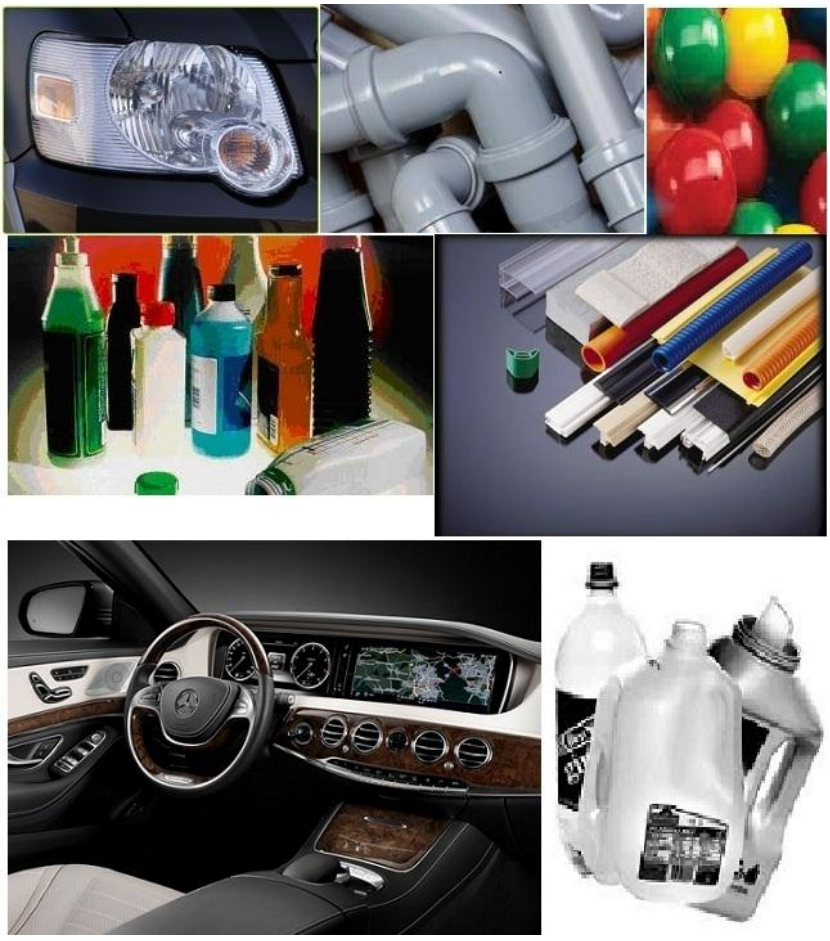

Figure1. 9: Applications of polymers for different products

1.5.2 Types of Polymers

A polymer is a compound consisting of long-chain molecules. It can be classified into two major groups [22]:

1. Thermoplastic polymers (thermoplastics)

2. Thermosetting polymers (thermosets)

1. Thermoplastic Polymers

Thermoplastic polymers become pliable or moldable above a specific temperature, and return to a solid state after cooling. Most of the thermoplastics have a high weight of molecular, due to of association chains through intermolecular forces; this property allows thermoplastics to be remolded because the intermolecular interactions spontaneously reform upon cooling [32].

The most important thermoplastics and their applications are as given below:

- Acrylics (Plexiglas):, window glazing, lenses
- Fluorocarbons (Teflon): seals, bearings
- Polyamides (Nylons, Kevlar): fibers
- Polycarbonates (Lexan): helmets, bullet-resistance windows, wind-shields
- Polyesters (Dacron, Mylar): gears, rollers, cams
- Polyvinylchloride (PVC): pipes, cable insulation, flooring, packaging , toys
- Polyethylene: packaging materials, cans, bottles,

2. Thermosetting Polymers

Thermosets polymers when heated at first time, become flow and soft for molding, but later they froze into an infusible solid. In fact, repeatable heating cycle is impossible for this kind of polymers.

The most important thermosets are:

- Epoxies: fiber-reinforced materials
- Polyesters: fiber-reinforced materials
- Silicones: waterproof and heat resistance materials

1.5.3 Conventional Manufacturing Processes for Polymers

1. Extrusion

In polymer extrusion, the feedstock is fed into an extrusion barrel where it is heated, melted, and forced to flow through a die opening by means of rotating screw (see figure 1.10)[33] :

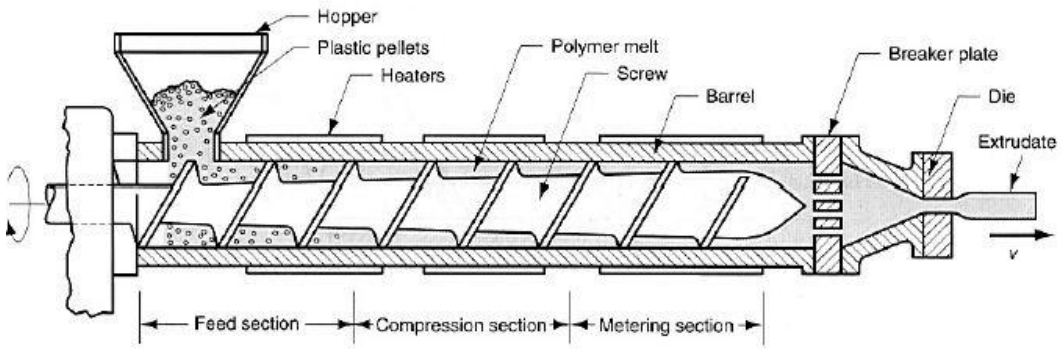

Figure1. 10: Components and features of a single-screw extruder for thermoplastics and elastomers

The raw materials not only in extrusion but also in most polymer processes are plastic pellets as can be seen in Figure 1.11:

Figure1. 11: Plastic pellets are the raw material in many shaping processes for polymer

2. Injection Molding

Injection Molding is a process, in which a polymer is heated to a highly plastic phase as shown in figure 1.12 .And forced to flow under pressure into a mold cavity, where it becomes solid. The component, called a molding, is then removed from the mold cavity: The production molding cycle time is in the range 10 to 30 sec. large parts with complex shapes are easily produced by injection molding [34].

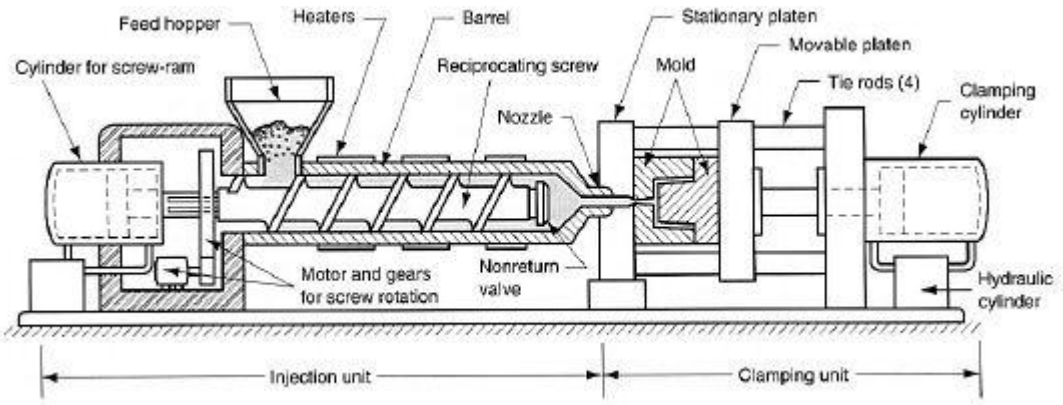

Figure1. 12: Diagram of an injection molding machine

3. Blow Molding

Blow molding is a modified extrusion and injection molding process, wherein a tube is extruded, clamped into a mold with a cavity much larger than the tube diameter, and then blown outward to fill the mold (as shown in figure 1.13). Blowing is done with a hot-air blast at a pressure of 350~700 KPa [34].

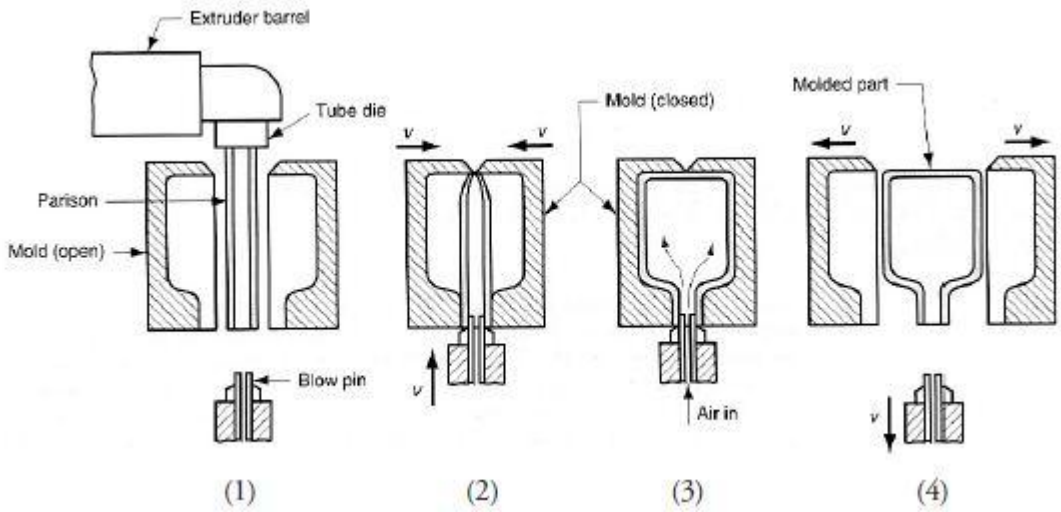

Figure1. 13: Blow molding process

1.5.7 Role of SPIF in Modern Process of Polymers

Polymers represent a significant percentage of the row materials utilized in industry but their processing technique use running on either melting or rubbery, are mainly suitable for mass production, because the energy cost and the capital investment in equipment and tooling are very high [23]. Likewise, injection-molding technology has conventionally expected general notice for the production of polymers parts. The cost-effective competitiveness of the process requires huge production batches to amortize the costs of dies and tooling [28]. As a result of this, conventional polymer processing technologies are not suitable for rapid product development and flexible small-batch production and, therefore not appropriate them for meeting the growing market trends on agile manufacturing. In this case of sheet polymer parts there is a lack of technology for making rapid prototyping the speedy process [29]. This technology should be for reducing and fixed the capital costs for reaching to the level where small-batch production with very short life-cycles and very short development and production lead times becomes economically feasible.

SPIF is an alternative technique, which is challengeable for current sheet polymer processing due to the necessity of creating innovative solutions that is capable of operating at room temperature with low tooling and equipment costs. For example, thermoplastic polymers, such like polyvinylchloride (PVC), polycarbonate, and polyethylene (PE), have revealed their ability to be formed to high strains by the single point incremental sheet forming process [23]. The formability of polymers with SPIF technology at room temperature makes this process as particular one. Because heating and cooling processes are omitted and therefore less energy and less equipment are required.

1.6 Objectives

Following are the objectives of the current study:

- The ability of the SPIF process to successfully form two polymer materials (PE and PVC) will be investigated.
- The forming limits of the above polymer materials will be determined and compared.
- The effect of variation in process parameters upon the formability of PVC and PE will be tested.
- The effect of temperature rise, as a result of parameter variation, on the formability of aforesaid polymers will be examined.

1.8 Organization of Thesis

This study is organized in five chapters in which each chapter are summarized as following:

The first chapter is an introduction about the ISF and its advantages and disadvantages. In addition, the application of ISF is explained in this section as well. The types of ISF process is described with its essential definition. Furthermore, formable materials are constructed for introducing some special materials which they can be used in ISF procedure. Then, the objectives of the thesis are summarized the investigation of two polymer sheets formability in SPIF (single point incremental forming).There are various view points of the scholars about the ISF and SPIF process that some of them are related to this study in the second chapter as the literature review. For SPIF process with polymers, equipment, procedures, and strategies of experiments are presented in Chapter3. The experimental equipment comprises forming tool, jig and fixture, lubrication, tensile test machine, CNC machine. Designs of experiment (DOE) are established for investigating the influence of processing parameters on formability of SPIF PE and PVC sheet, feed-rate, step size, spindle speed and tool diameter are considered in an experimental strategy.

The experimental procedures and experimental analysis for polymeric material are presented in chapter 4. The Tensile test is performed on polymer sheets. Then, for understanding about mechanical behaviors more clearly, their microstructure is examined. Also, the analysis of the effect of process parameters upon the temperature and formability of PE and PVC sheets is explored in this chapter.

The results of SPIF process with two kinds of polymer sheets (PE & PVC) are summarized in the last chapter. Moreover, the suggestion for further research is observed in chapter 5 as the final section.

Chapter 2

LITERATURE REVIEW

2.1 Scientific Background on SPIF

In 2001, the investigation on SPIF was flourished to prospect its ability to perform die-less forming [2]. Since 2001, the number of the researches has been focused on different aspects of single point incremental forming, to extent it for industrial application. Now, in this section the summary of the previous works is introduced.

2.1.1 Equipment and Tooling of SPIF:

In order to perform SPIF process, ordinary 3-axis CNC milling machine can be applied. Such machines are designed as multi-purpose machines in which both machining and forming processing can be done. So, the new design of SPIF machines is also being recommended to modify the performance of method. For instance, one-off design by Allwood [15], which is lately proposed SPIF machine. For having automated process fully, robots are applied to incremental forming by some organizations investigations [39].

Normally, a tool with spherical/hemispherical end in a shape of steel rod is applied as a forming tool. Plastic tools and cemented carbide were tried by Hirt [40]. He indicated that tools which are made in cemented carbide have the ability of reducing sheet/tool interface friction, hence improving surface quality. The SPIF tool can be held in a stationary or rotating spindle .Tool size selection be influenced by upon the

size of component: the tool radius ranging is from 3-50 mm has been applied to form various size components.

2.1.2 Surface Quality:

According to Jeswiet et al [18]. Investigations in step size and tool radius which are affecting roughness of the surface are the main process parameters. Also it has been accounted that R_z (mean peak to valley height) in comparison with R_a (average roughness) is more useful measurement of surface roughness in SPIF. Afterwards, Junk et al. studied the interactive influence of wall angle, step size, and tool size [41]. They revealed that the interaction of studied parameters directly effects on the roughness of the surface, and the appropriate combination of these factors can be produce components with the quality of sound surface. Jeswiet and Hagan explored that during forming samples, with using of SPIF the unsupported surface of the part is affected by an unpleasant phenomenon as orange peel effect, while the forming process is performed with large wall angle [2].

2.1.3 Forming Forces:

Requirement of the force to form a sheet is an initial approach for machine designers. The pioneering research in this area was performed by Jeswiet and Nyahumwa [42], they measured forming force for TPIF method by applying a cantilever sensor. After wards, in order to illustrate that force increasing depends on the wall angle increasing, Jeswiet and his co-workers measured forces in SPIF, in which Duflou et al[43] carried out more advanced research in this case. Therefore, the effect of 4 parameters in SPIF process, namely tool radius, sheet thickness, wall angle, and step size was investigated by them. For measuring forces, they used six part force dynamometer. It was explored that increasing in any of the studied parameters, causes forming force an increase.

According to the influence of wall angle, the important finding was described: when the wall angle is in the maximum accessible, a peak which is following by a dip in force happens. It is supposed as a pioneer of sheet fracture. Ambrogio et al. [17] showed that by declining the tool size and step size, the peak height can be decreased. Regarding this finding, a strategy for avoiding premature failure was proposed by them.

2.2. Forming limits

2.2.1 Wall Thickness and Sine Law*:*

Jeswiet and Young [44] performed the investigations upon wall thickness in SPIF. They formed a number of cones with a diversity of wall angles (θ as showed in Fig. 1.6) and also found that when wall angle is minor, the sine law is suitable. While the wall angle is increasing, a thinning band happens as illustrated in Fig. 2.1. The sine law's prediction is larger than the wall thickness in this band. Additionally, they mentioned that the testable thickness of minor wall angles, for example 30°, lies a little under the sine law's predictability and difference between the testable thickness and sine law's expect, thickness in thinning strip , decreases when the wall angle increases.

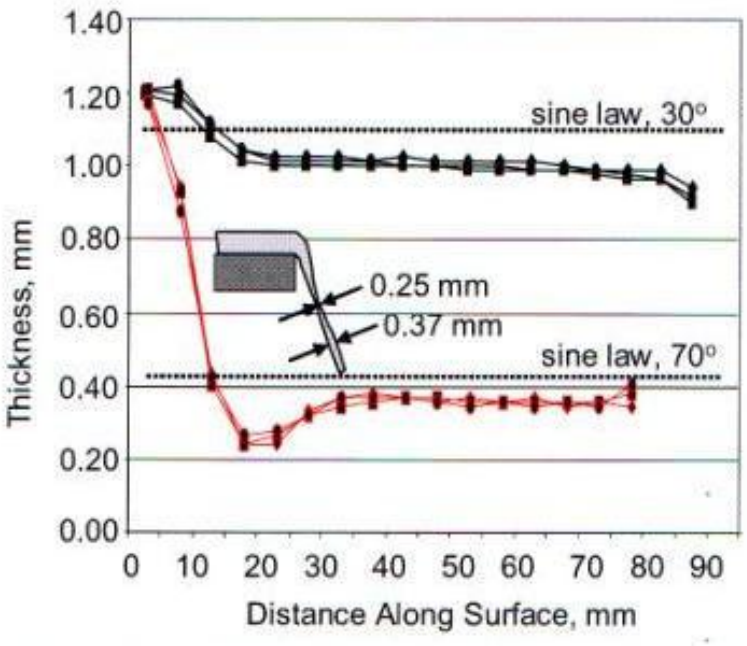

Figure2. 1: Wall thickness indexes for 30o and 70o cones [47]

Also, conducting experiments to study distribute of thickness in SPIF were carried out by Wei and Gao [47]. They formed irregular complex forms and found that the wall thickness followed the equation below:

$$t = t_0 \cos\theta \tag{1.4}$$

Where

t equals the final thickness of the wall

t_o equals the original blank thickness

θ equals the wall angle

According to the Figure 2.1, it can be stated that Eq. 1.4 is another type of sine law. Nevertheless, owing to usage of wall angle (θ) in place of half apex angle α this equation is a cosine function. The Eq. 1.4 was named as a cosine law. In this study, everywhere needed, cosine law will be utilized for wall thickness predictabilities.

2.2.3 Representation and Evaluation of Formability

In SPIF process, since the wall thickness decreases as the wall angle increases [44], the fracture of sheet will happen when the thinning limit is outstrip. Hence, there is a maximum amount of wall angle that a sheet can tolerate devoid of fracturing. This angle is so-called maximum wall angle θ_{max} in SPIF method and all the scholars are approved upon utilizing maximum angle of wall to calculate formability term in SPIF [30, 41, and 45]. The shape normally utilized to specified maximum angle of the wall is frustum of cone. For evaluating maximum angle of the wall, frustum wall angle is raised in small stages till the maximum value is achieved devoid of fracturing.

A number of researchers have specified forming limit curve (FLC) in the minor -major space of strain to present formability in SPIF. Kumon and Iseki [86] represented that FLC may seem as a straightforward direction with negative incline in tension-tension quarter of the forming limit curve. Later Park [21] also stated the same conclusion. Jeswiet [18] put forward a forming limit figure to project the formability of a diversity of complex shaps.

Huang et al proposed FEA method to project formability in SPIF. [48]. A ductile directorial model of fracture, which consists of the efficacy of hydrostatic stress on the happening of the fracture, suggested by Oyane et al. [49] was selected. Through performing straight groove testing analytically and experimentally, they discovered that the model of fracturing can be efficiently utilized for the mentioned object.

2.2.4 Formability and Process Parameters:

The formability in SPIF can be affected by several parameters. Considering other parameters fixed, Jeswiet et al. [44] investigated the influence of sheet thickness, they found that as the sheet thickness increases, the formability of aluminum sheet increases in a linearly mode. This true was found for DCO4 steel sheets by Hirt [41] as well. Upon the formability, Park and Kim studied the effect of 4 various parameters namely, tool size, step size, tool type , friction at the sheet/tool interface and plane anisotropy of sheet component . The following results were reported: The ball shaped tool is conducive for modifying formability in contrast with spherical tool; for favorable formability, large values of step size and tool size and are not suitable; a little amount of friction takes down the stress state and has a positive influence on the formability, however, big amount of friction causes sheet wear and therefore decrease in formability. Also, Micari [46] searched on the effect of tool size and step size and discovered that the formability reduces as a direct result of increasing these two factors. This issue has been also found by Hirt et al. [40] they carried out finite element analysis (FEA), in order to find the effect of step size on the formability. And also showed that increasing in formability is because of reducing in step size due to declining in mean stress amount in part's wall.

Jeswiet et al. [18] have showed that increasing forming speed in a linear situation cause a negative influence on the formability. They have been found that increasing in spindle speed having a positive effect on the formability as a consequence of increasing in heating at the sheet/tool interface.

2.3 Numerical Analysis

Some scholars have tried to progress analytical computations to calculate different amounts related to the SPIF method. Some of these forecasts are explained as following: developing deformation analysis study of the bulging height for predicting strain in SPIF and multistage SPIF method was carried out by iseki [51]. To propose the strain dispensation and forming load of the shell, the researcher was applied a FLD and deformation model for plane-strain.

Pohlak [50] explored statistical analysis for forming force according to a simplified theoretic model to approximate the force components performed by Iseki. The author also took account of influences on anisotropic behavior of materials. The values of the forming load and its ratio, and components, corresponding to theoretic and empirical models were discovered.

Duflou et al. [43] studied an interaction between the primary processing parameter (stool radius, depth step, sheet thickness, wall angle) and forming force by applying design of experiment analysis method (DOE). From this DOE, a reversal equation of forming force and the parameters of process is elicited to expect the forming force for other complex profiles in SPIF method. This work was continued and developed for five types of material by Aerens et al et al.[52]. They took a potential reversal model which allowed calculating the tangential and axial components of the forming force in a stable state with a proper accuracy. Furthermore, for evaluating the analysis again, they applied FEM simulation.

Filice et al. [17] developed a new control and monitoring method for controlling the most process parameters during the operation of SPIF in an online condition. So, a set of primary experiments for evaluating the influence of single process parameters on a tangential force orientation. Therefore, a numerical analysis was applied to acquire a relationship between the process factors known as ‘’variable of spy”. The importance of this correlation is because of the fact that the ability of performance to control strategies which allowed to expect the force gradient.

Martins et al. [13] applied membrane analysis to extend a theoretical model of SPIF. With respect to the three main modes of deformation the stress and strain state is separated into three kinds: 1) smooth surface below plane stretching strain conditions; 2) rotating symmetric surfaces beneath plane stretching strain states; 3) corners below equal bi-axial expanding conditions. According to this investigation, the researchers can clarify high formability, hydrostatic stress, stress-strain state, and mechanical fracture…etc.

2.4 Formable Material Used in SPIF

2.4.1 SPIF Process with Magnesium Alloy Sheet

The SPIF technique represented a flexible manufacturing method .This method promises the possible practical applications for lightweight metals according to larger design potentials and work hardening increasing. Currently, there are the attempts to utilize this method for magnesium AZ31 sheet. The first research on SPIF method for magnesium AZ31 sheets carried out by Ambrogio et al [19]. A forming space with an insulation and heating system is designed to reach an effective thermic control on the sheet, preventing thermic gradients. The study concentrated on the determination of the formability limitations of AZ31 as well as the relationships

between process parameters and formability by applying a good design of experiments (DOE). The tests were carried out in temperature limits of 200-300°C to measure the influences of step size, tool diameter, and forming temperature. The experiments concluded that formability improvement is conceivable working magnesium in warm states. The effects of tool step size and temperature and on formability are fully important, while the effect of tool diameter is insignificant. Ji et al. [21] studied the SPIF process for AZ31 sheet with great range of temperature (100-250°C) while the maximum formability attained at 250°C.

The introductory stretching experiments were carried out to evaluate the effects of temperature to the axisymmetric strain and forming limits in plane at the temperature among the ranges of (20- 250C). The conclusion also represented that the increasing of formability of AZ31 sheet occurs as the increasing temperature in SPIF. Then, the SPIF tests and FEM simulation of this processing applied in a cone-shaped model with different temperatures. The researchers recommended the conception of progressive forming which permitted exceeding the forming limits in deformation of a circular-shape cup with a great inclination angle.

Zhang et al. [37] investigated the effects of manufacturing approach on the mechanic anisotropy of magnesium sheet with SPIF. This research focused to the four types of magnesium sheet which is manufactured by various methods. The manufactured methods including of strip-casting rolling, cross rolling, slab-hot/cold rolling, and hot extrusion. The results of this study stated that the cross-rolled casted and slab-hot/cold rolled sheets with the size of grain amount 5–15μm are not the considerable anisotropy. The others are significantly affected on formability by behavior of anisotropic, but it diminished the influence of anisotropy while the

forming temperature increased. Also, the authors suggested that cross-rolling sheets are much more proper for warm SPIF method. The quality of surface of incremental formed components is principally depended on step size and the lubricated states. The lubrication methods were examined to decline the friction between sheet surface and forming tool in negative SPIF with magnesium alloy sheets. The researchers tested SPIF process with AZ31 in various lubricating approaches such as solid graphite, Nano-K2Ti 409 and MoS2. They are employed under a pulsed anodic oxidation and lubricant film in SPIF method with AZ31 sheet. According to the results, the sheets with a pulsed anodic oxidation treatment in SPIF process have proper quality of surface. The Nano-K2Ti409 whisker lubricating in the combination of M0S2 or single solid graphite which has a coefficient around 0.07-0.10. It fulfilled with the friction and lubrication states of SPIF of the sheet and giving the finest quality of surface.

2.4.2 Titanium

Biomedical and Aerospace applications are being more used in the past. Tanaka et al. [36] showed the viability of the SPIF processing of unalloyed titanium in an application of denture plate, the major problems in the production of this component were the quality of surface, requiring discovering optimal combination between lubrication and feed rate. Hussain et al. [45] stated that if a, proper tool, and lubrication method is employed, SPIF can also be used in commercially pure titanium.

2.4.3 Composites and Polymers

As discussed in the previous sections, a great deal of work has been performed on metallic materials. In addition to metallic materials, some studies have been done on

non-metallic materials as well. This work is, however, is very limited, as summarized below:

Jackson et al. [25] utilized SPIF on a typical sandwich panel with three layers of metal-polymer-metal. Four sandwich panels were examined to investigate mechanical viability of SPIF processing with sandwich panels. They performed for a huge range of sandwich panels' properties which were accessible in the industrial applications. The primary tests applied a straight path (100 m) and short spiral tool path (step size of 0.1 mm) for considering the decline in thickness, mechanical failure and degradation of the quality of surface after deformation. The scholars concluded that SPIF processing could employ properly on sandwich panels with construction of Aluminum- polypropylene- Aluminum and Mild steel-polypropylene-Mild steel because of having high ductile and mostly faceplates and incompressible core. The states of the sine low and through-thickness strains explain thinning of sheet with wall angle are like sheet metal. The vertical forcing of tool represents similar differences with vertical pitch and tool radius.

Franzen et al. [28] applied the tests on polyvinylchloride (PVC) with using ISF method. To investigate the formability of PVC, a conical-shaped component is employed. The researchers showed three kinds of mechanical failure happened in forming processing. The amounts of the maximum wall angle (θ_{max}) obtained in forming process of PVC differ between 67 and 72. The authors tried to overcome 'stress whitening' phenomenon which altered the color of forming component. As regards, the obtained findings look to be unexpected.

Martins et al. [23] investigated on five kinds of polymers to focus on the specification of processing limit and the properties of product evaluation. So, by

means of tensile and bi-axial tests the formability of polymers sheets with SPIF process was investigated. From those tests, PVC s' forming limit diagram is recognized. A DOE planning is designed with four parameters (tool radius, sheet thickness, initial drawing angle and kind of polymer material) in a full factional method to investigate the formability of polymer components.

The work on polymers is not adequate to deploy the SPIF process in industry. So, further work is required to attain more knowledge to successfully implement SPIF for manufacturing of polymer components. Therefore, further work has been performed in the current research, details of which have been provided in the next chapters.

Chapter 3

MATERIALS AND METHODS

3.1. Materials and Their Mechanical Properties:

Two kinds of polymeric material are selected in current study .These are polyvinylchloride (PVC) and polyethylene (PE) (see Figure 3.1). The thickness of these materials is about 2mm. The physical properties of mentioned materials are presented in table 3.1[23].

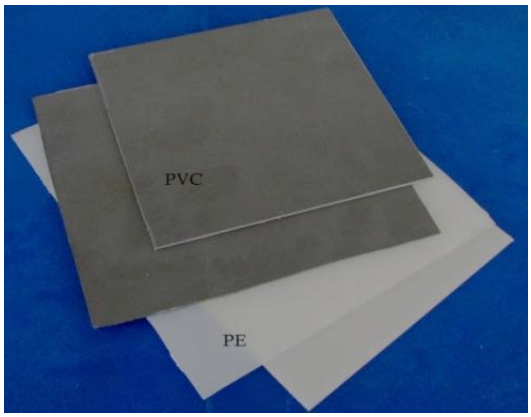

Figure3. 1: PVC and PE sheets

Table3. 1: The summary of physical properties' of polymers sheets (PVC and PE)

Material type	Structure	Density (kg/m^3)	Melting point (c°)
PE	M-C	966	115
PVC	L-C	1469	180

In order to test the mechanical properties of polymer sheets, tensile samples were produced along 0°and 90° directions to the sheet rolling direction [26]. The samples were cut using CNC milling machine according to ASTM A370 standard (see figure

3.2 and Table 3.1). Tests were performed by using Instron 3385 tensile testing machine at tensile test laboratory of Middle East technical university, as shown in figure 3.3. The samples were stretched to fracture.

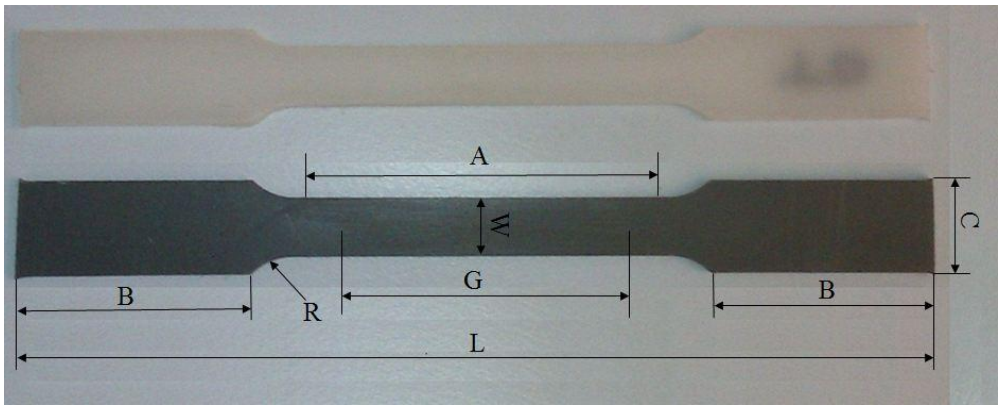

Figure3. 2: Tensile test specimens using ASTM A370 standard

Table3. 2: ASTM-A370 standard dimensions

ASTM A370 Standard Dimensions			
G—Gauge length	50 ±0.1 mm	*A*—Length of reduced section	60 mm
W—Width	12.5 ±0.25 mm	*B*—grip section Length,	50 mm
R—Radius of fillet	13 mm	*C*— grip section Width,	20 mm
L—Overall length	200 mm	*T*—Thickness	2 mm

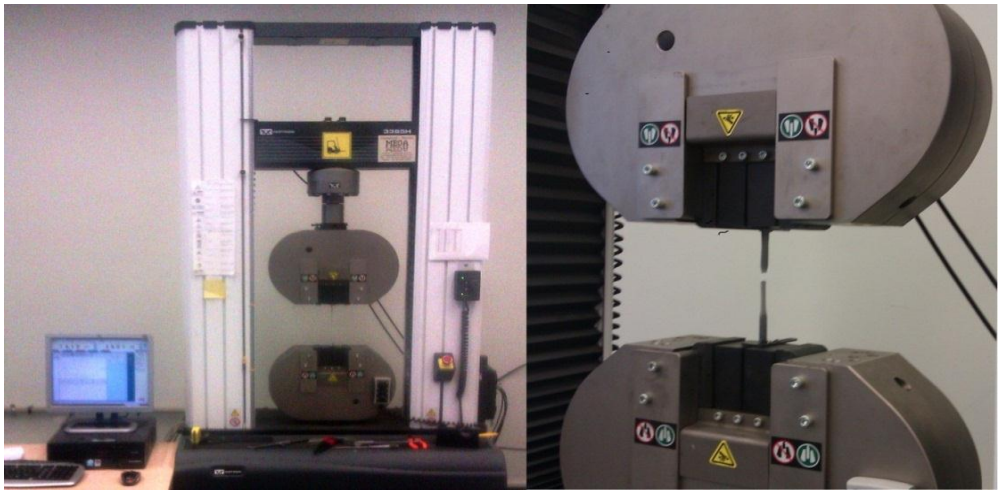
Figure3. 3: Instron 3385 tensile test machine

To calculate the mechanical properties of polymer sheets, stress- strain curve for each sheet was drawn (shown in appendix 1). The percentage reduction in area at tensile fracture (A_r) and percentage elongations (%E) were computed using the following formulas:

$$A_r = 100 \times (A_o - A_f)/A_o = 100 \times [\{(w_o \times t_o) - (w_f \times t_f)\}]/(w_o \times t_o) \quad (3.1)$$

Where

A_r is the percentage reduction in area

A_o is the initial area of cross section of the tension test sample

A_f is the area of cross section at the fracture of sample

A_o is determined by measuring the original thickness (t_o) and width (w_o) of the test sample. And, A_f was calculated by measuring of the minimum thickness (t_f) and minimum width (w_f) at neck of fracturing, as shown in Figure 3.4. Thickness and width were measured using digital vernier calipers to an accuracy of ± 0.01mm.

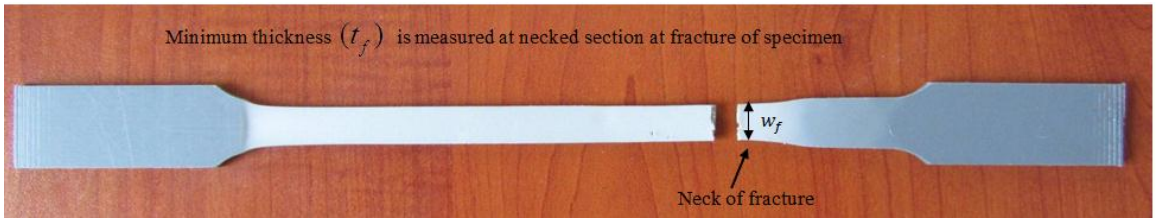

Figure3. 4: Explanation of the method applied for measuring thickness and width at fracture of a tension test specimen

The percentage elongation (%E) was calculated as follows:

$$\%E = 100 \times (l - l_0)/l_0 \quad (3.2)$$

Where %E is percentage elongation, l is the final length of test specimen and l_0 is the original length of tensile specimen.

The important tensile properties are shown in Table 3.3. As can be seen, PVC has high strength and ductility (elongation and area reduction) than those of PE.

Table3. 3:.Summary of mechanical properties of PE and PVS sheets

Type of material	σ_y (Mpa)	σ_{UTS} (MPa)	%E	A_r
PE	5.0125	17.6641	97.72%	85.56
PVC	15.125	47.6348	29.22%	55.49

3.2 Test geometry

3.3.1 Major Concept of The Test

As mentioned in chapter 2, the final wall thickness in SPIF depends on the wall angle (also called deformation angle) imposed and can be predicted utilizing the cosine law [44] as follows:

$$t = t_o.cos\theta \tag{3.3}$$

Where

t equals to final thickness of wall

t_o equals to original blank thickness

θ equals to the angle of wall

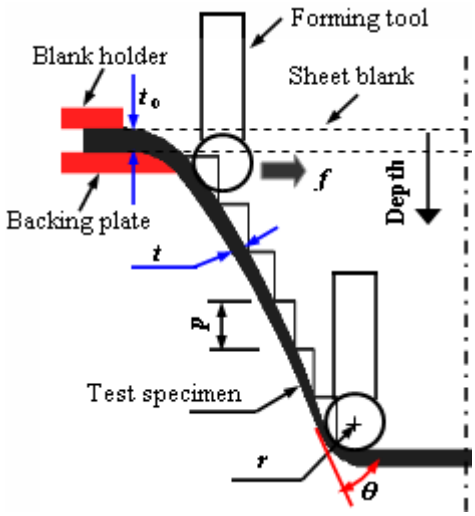

Figure3. 5: Schematic view of a part with continually changing wall angle

According to the cosine formulae, wall thickness of a component with deformation angle continually increasing can be proposed as shown in Figure. 3.5. The cosine law

can predicts that thinning of wall angle along the part depth will rise with increasing in wall angle, and also, 90° wall angle may not be formed fruitfully. Hence, if the wall angle varied from 0°–90° as shown in Fig 3.8, fracturing of sheet will happen among 0° and 90° whenever the sheet thinning limit is outstripped . Regarding this indication, a shape, as revealed in Fig 3.5 with continually changing wall angle was planned and the test of formability was carried out on it. The mathematical equations and the method of obtaining the maximum deformation angle are explained in the next sections [26].

3.3.2. Test Geometry and Mathematical Equations:

Figure3.6 illustrations the test geometry selected for testing formability of polymers [13].For generating the test geometry the arc MN of a circle was applied as generatrix the description of the symbols shown in the geometry is outlined below:

$f(x_f , z_f)$ The point at which sheet failure (fracture or wrinkling) is expected to occur

R Radius of generatrix or circle

h_f Depth of surface measured to failure point

θ_f Final wall angle of generatrix

If θ_f is the wall angle at the failure point $f(x_f , z_f)$ its value can be computed

In terms of known quantities such as h_f and *R*. making use of *Δ FOP* in Figure 3.6,

$$\theta_f = cos^{-1}(z_f / R) \quad (3.4)$$

$$= cos^{-1}((Z_m - h_f)/ R))$$

Here R and Z_m are constants and can find from test geometry dimensions. Additionally, h_f can be measured directly from a formed test specimen. Eq.3.4 will provide an ease in computing wall angle at any point on a formed test specimen.

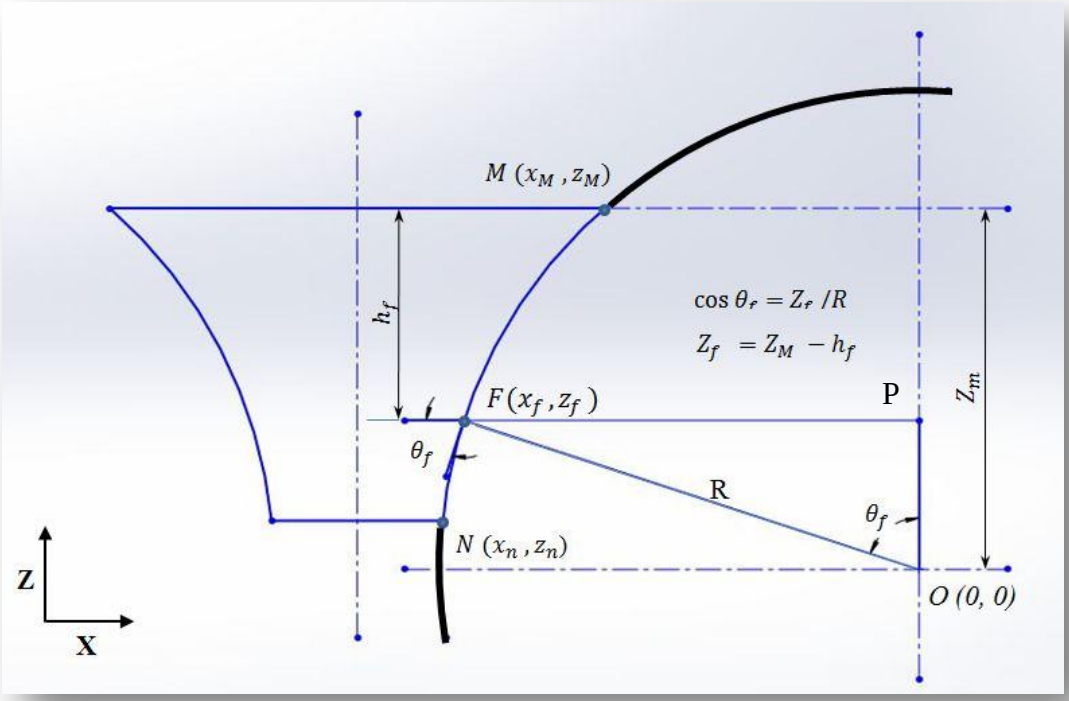

Figure3. 6: Description of Terminology and Test geometry

The geometrical details of the test performed to test the formability of polymer sheets are shown in figure 3.7. This test geometry (i.e., frustum of cone having varying wall angle) was designed in commercial Solid works software. The forming angle value (i.e.θ_f) was changed from 60° to 90° in the tests.

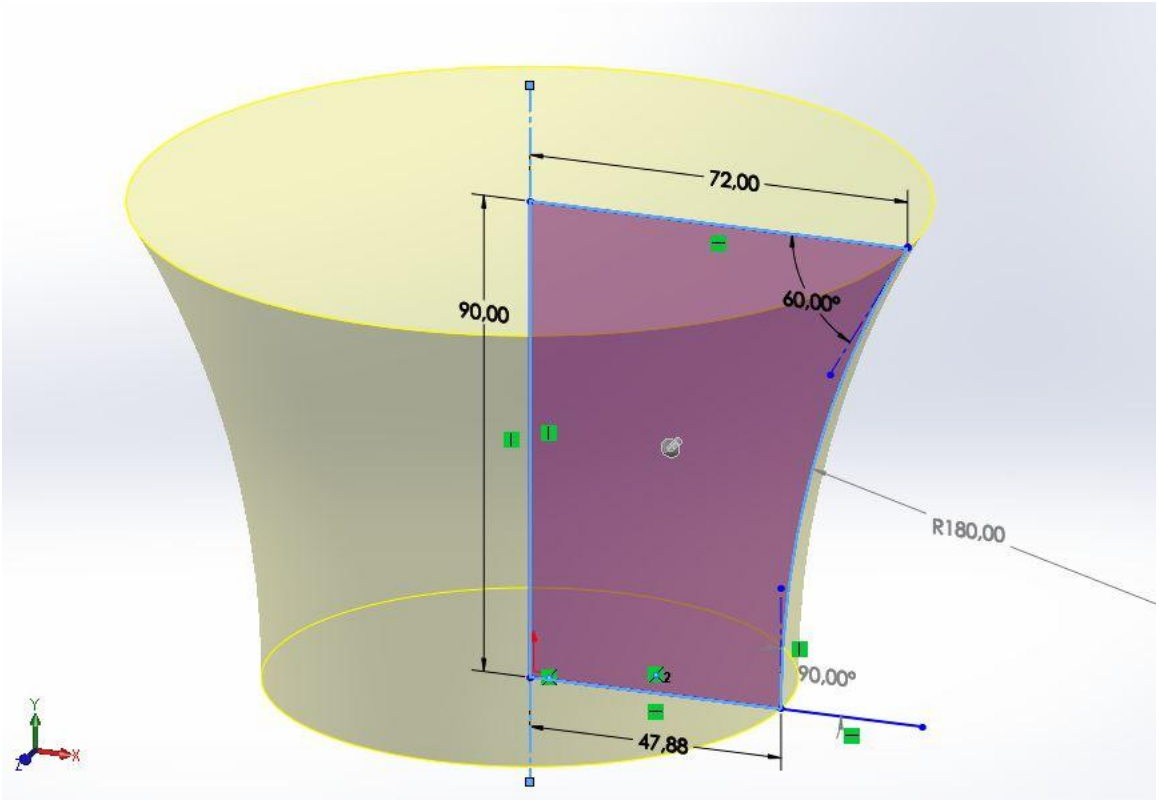

Figure3. 7: 3D view of Geometrical details (in mm) of the formability test performed on the frustum of cone with continuously varying wall angle.

3.4 Formability Calculation

Generally, the maximum wall angle, denoted by ($\theta_{\max}$) is defined as: the maximum value of wall angle that a sheet would endure without failure (fracturing or wrinkling). The wall angle continuously increases from the initial point M (x_m ,z_m) to the final point N (x_n ,z_n) of test geometry. And, the fracture or wrinkling will occur somewhere between these two points. Therefore, the wall angle at failure point can be regarded as the maximum wall angle ($\theta_{\max}$).The formability of polymer sheets in SPIF can be defined in terms' of maximum wall angle reached without failure[23]. This angle was measured at position where the mechanical failure of the deformed sheet occurred. For calculating maximum wall angle The Eq. 3.4 can be re-written as below [26]:

$$\theta_{\max} = cos^{-1}((Z_m - h_f)/R)) \quad (3.5)$$

Where h_f is the depth of test specimen measured to failure point $f(x_f, z_f)$.

3.6 Test Plan

To study the effect of operating parameters and their interactions in SPIF upon the temperature and formability, statistical designs were prepared and D-optimal method of designs was used [30]. Test parameters were arranged in fractional mode to study their closer correlations in order to find the proper selection and reducing the number of runs as shown in Table 3.4.

The design was based on response surface methodology and was prepared in twenty runs (see Table 3.5). Response surface is a methodology based on statistical method for process control and optimization [45]. The maximum wall angle ($\theta_{\max-f}$) at fracture and wrinkling point ($\theta_{\max-w}$), in addition temperature, obtained in SPIF process are considered as responding parameters of DOE. Furthermore, the designs and all required statistical analyses were performed using a commercial computing package, known as Design Expert dx-8.

Table3. 4: Parameters and their low and high levels

Parameters of designed experiments	Low level	High level
Tool radius / Sheet thickness (r/t_o)	2	5
Tool radius / Step size (r/p)	3.33	10
Spindle speed / Feed rate (w/f)	0.01	0.8

Table3. 5: Design of experiments

Run	Factor 1 A: (r/t_o)	Factor 2 B: (r/p)	Factor 3 C: (ω/f)	Factor 4 Material type
1	3.50	10.00	0.01	PVC
2	5.00	10.00	0.40	PE
3	2.00	6.67	0.01	PVC
4	2.00	6.67	0.01	PE
5	3.50	10.00	0.80	PVC
6	2.00	6.67	0.80	PE
7	3.50	3.33	0.01	PVC
8	3.50	6.67	0.40	PE
9	2.00	3.33	0.40	PVC
10	3.50	6.67	0.40	PE
11	2.00	10.00	0.40	PE
12	5.00	3.33	0.40	PE
13	2.00	6.67	0.80	PE
14	2.00	10.00	0.40	PVC
15	3.50	3.33	0.01	PE
16	2.00	3.33	0.40	PE
17	5.00	6.67	0.01	PE
18	5.00	6.67	0.01	PE
19	5.00	6.67	0.80	PVC
20	3.50	3.33	0.80	PVC

3.7 CAD and CAM:

The SPIF process extensively makes use of commercial CAD/CAM software for part modeling and tool path generation. Many commercial CAD/CAM packages are available to serve the intended purpose. The package employed here, however, was solid works. The part geometry of any product to be produced was generated in the CAD module of solid works and the tool path from the CAD model was generated using the CAM module. Spiraling tool path is employed to investigate SPIF of polymer sheets. Figure 3.8 shows the mentioned tool path generated for a conical frustum. In this kind of tool path the height of contour continuously changes in the plane perpendicular to tool axis. [26]

`

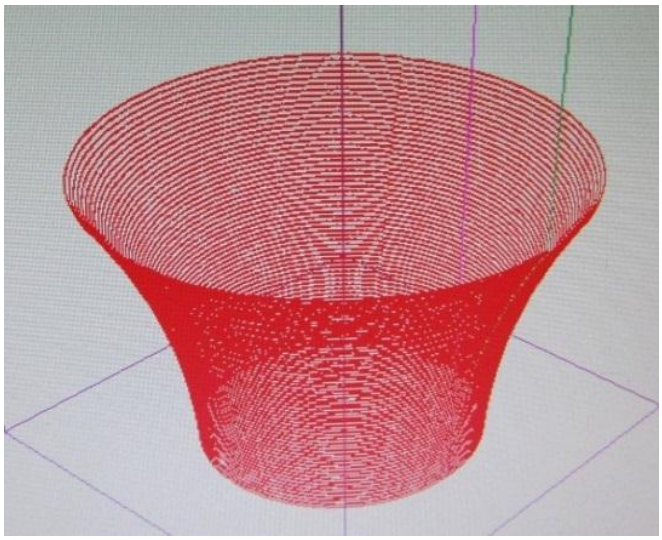

Figure3. 8: spiraling tool paths: Forming begins from top to bottom

3.8 Incremental Forming Setup

3.8.1 CNC Machine

For forming the tests specimens' 3-axes CNC milling machine (Dugard Eagle 760) was employed [13, 15]. The tests were performed at CNC laboratory of Mechanical Engineering Department in EMU (Eastern Mediterranean University) as shown in Figure 3.9.

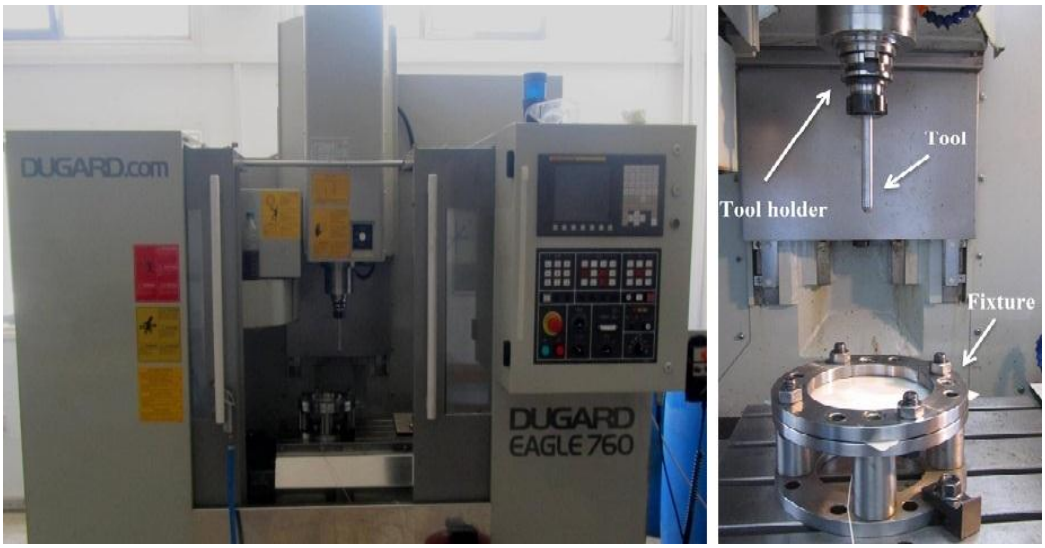

Figure3. 9: CNC milling machine

The parameters of the mentioned CNC machine are listed in Table 3.6 and the utilized equipment's were described in the following section.

Table3. 6: CNC milling Machine Technical Specifications

CNC Operating System	Fanuc Series Oi-MD
Number of Axis	3
Machining capacity (mm)	760× 430×460
Max. Tool Diameter (mm)	89
Max. spindle speed (rpm)	8000

3.8.2 Tooling:

A forming tool for SPIF process of polymeric materials is a solid hemisphere head that made from high speed steel (HSS) with hardness of 60–65HRC. The tools were designed with straight shank and three kind's tools with diameter of 8,14and 20 mm are utilized. See figure 3.10 [41].

Figure3. 10: Forming tools for SPIF

3.8.3 Clamping Mechanism

The rig to clamp sheet blank was made of steel. It was composed of blank holder, backing plate and a base frame. A backing plate is used to decrease spring-back problems in deforming process. Moreover, the sheet blank was tightly held at the periphery with the blank holder. All components were connected together by bolts and are clamped firmly on the CNC machine table as revealed in figure 3.11. [13].

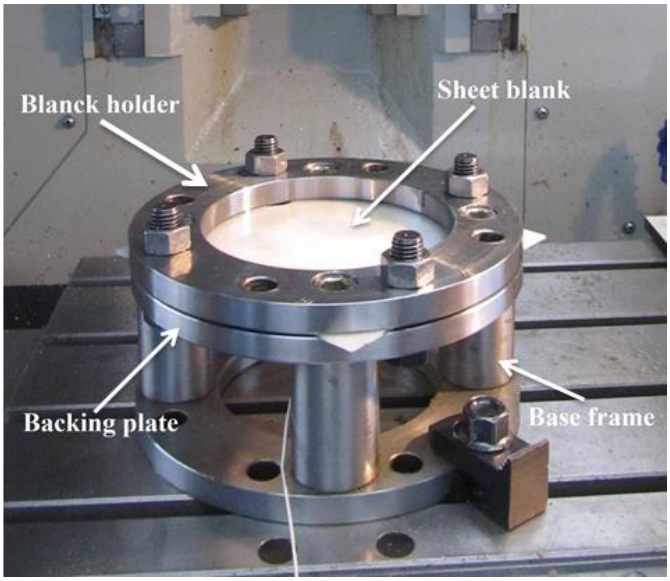

Figure3. 11: Clamping system of polymers sheets

3.8.4 Lubrication

The forming tool has the end-hemispherical shape, which is pressed into the sheet to cause the locally plastic deformation. The heat due to friction and wear of tool increases highly during the tool movement. Tool wearing and local heating influenced on the surface quality, formability and the geometric accuracy. In order to decrease those effects, different lubrications need to be used for different types of deforming material. Zhang [37] have been investigated the suitable lubrications and lubricating methods. For polymeric materials, the friction between the surface of sheet and the tool is relative high. The local heating can exceed the softening temperature of the thermoplastic polymer. In this case, the formability of SPIF process increases but the deformation of sheet is not stable. In order to avoid this effect, machine oil is used in this study for SPIF with polymer materials.

3.9 Measurement of Results

3.9.1 Formability Measurement

The square sheet blank was held tightly between the upper and lower plates with the use of fixture; in addition, all components were fixed on CNC machine table as can

be seen in figure 3.11. The forming tool was positioned onto the sheet in such a way that the center of CAD geometry and that of the clamping plates coincided. The downward and rotational movement of the forming tool deformed the sheet progressively and the formability test continued till the failure of sheet occurs [26]. The machine tool was stopped manually as soon as the fracture occurred. And the depth of specimen corresponding to fracture point $f(x_f, z_f)$ i.e.,h_f can be measured by fixing the formed part with fixture (see figure 3.12). The measurements were carried out with a depth gauge to an accuracy of ± 0.01mm.the measured values of h_f was later put into Eq. 3.5 to compute maximum wall angle. Moreover, the depth of specimen related to wrinkling point which was found to happen before fracturing in polyethylene (PE) SPIF, gotten from z-value of CNC machine in the time of occurrence as can be seen in figure 3.13. In addition formability corresponding to wrinkling point was calculated similarly to fracture point [23].

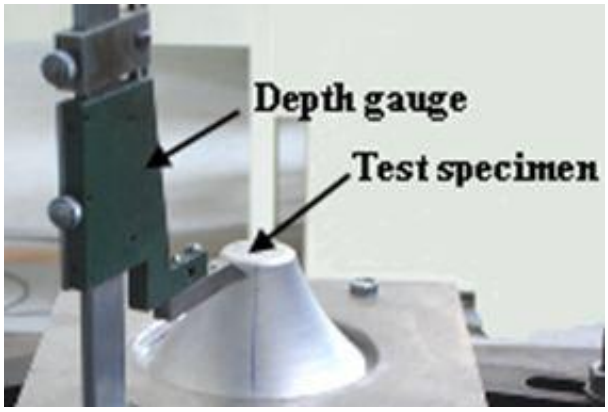

Figure3. 12: Method of measuring depth of fracture

Figure3. 13: Z-value gotten from CNC machine

3.9.3 Temperature Measurement

As illustrated in figure 3.14, for evaluating the influence of operating parameters in SPIF of polymers (PVC and PE) the temperature measuring was employed during the experiments with help of the digital thermometer device (Xplorer GLX) with a wired sensor. Furthermore, the sensor was attached to the bottom of sheet blank using silicon glue. This kind of device has the capability to reveal the increasing temperature by means of graphs and numbers step by step.

Figure3. 14: Digital Thermometer device

Chapter 4

RESULTS AND DISCUSSION

In the present chapter, the influence of operating parameters of SPIF process upon the temperature and formability of polymers sheets (PVC and PE) will be discussed. Moreover, regression analysis and an empirical model describing the effect of parameters [45] on temperature and formability for each mentioned material will be developed. The results will be analyzed and optimized with the help of Design Expert-8 software.

4.1. Temperature

Based on the SPIF mechanism [15], a variation in operating parameters in SPIF process influence the temperature at the tool/sheet contact, most probably as a result of change in contact area and forming time. The temperature, as mentioned before in the preceding chapter, was measured using a digital thermometer (Xplorer GLX) and (according to table 3.1 in chapter 3) softening trend of each of PVC and PE was obtained by dividing the measured temperature by the melting point (*mp*) of respective material, as follows:

$$\Delta t/mp \tag{4.1}$$

4.1.2. Regression Analysis: Significance of Operating Parameter for Temperature

Figure 4.1 shows the results of temperature tests. As can be seen from the Figure that the maximum temperature rise (i.e., $\Delta t/mp$) occurs in PE (0.2086) and the minimum one occurs in PVC (0.10437).

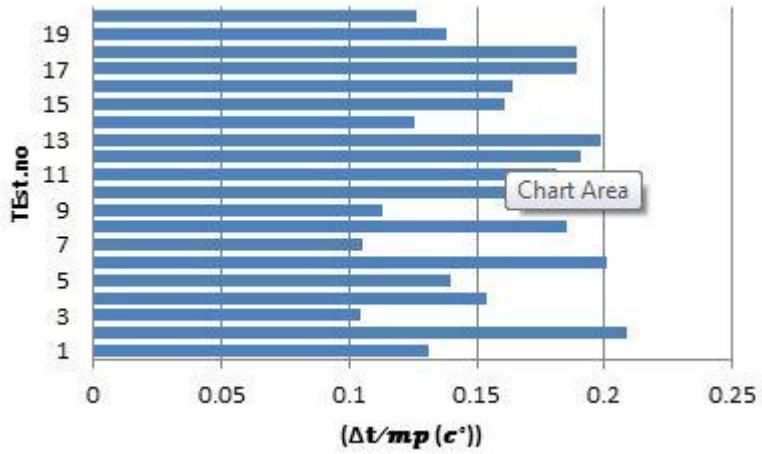

Figure4. 1: Results of (Δt⁄mp (c°)) tests

In order to find the significant parameters affecting temperature rise, regression analysis was done with the help of Design Expert software [30]. In the beginning, as the software suggested the 2FI model was selected. The summary of ANOVA (analysis of variance) of the model is shown in Table 4.1. The terms with P-value (or probability) ≤ 0.05 was considered significant. It is obvious from the table that the model is significant and the parameters such as r/t_o , $r/p, \omega$ / f and D (type of material), in addition the interactions such as ω/f D, $r/t_o\ \omega/f, r/p\ \omega/f$ and r/t_oD are also important. Based on P-value, the order of significance of terms is given as follows:

D (type of material) > ω/f > r/t_o > r/p > ω/f D > $r/t_o\ \omega/f$ > $r/p\ \omega/f$ > r/t_oD

Table4. 1: Summary of ANOVA response surface 2FI model ($\Delta t/mp$ (c°))

Source	Sum of Squares	df	Mean Square	F Value	p-value Prob > F	significance
Model	0.022	10	2.246E-003	350.22	< 0.0001	significant
A:r/to	8.437E-004	1	8.437E-004	131.53	< 0.0001	significant
B:r/p	7.427E-004	1	7.427E-004	115.79	< 0.0001	significant
C:ω/f	1.257E-003	1	1.257E-003	195.98	< 0.0001	significant
D:M.t	0.011	1	0.011	1778.61	< 0.0001	significant
AB	6.021E-006	1	6.021E-006	0.94	0.3579	
AC	1.655E-004	1	1.655E-004	25.80	0.0007	significant
AD	3.362E-005	1	3.362E-005	5.24	0.0478	significant
BC	3.608E-005	1	3.608E-005	5.62	0.0418	significant
BD	8.105E-007	1	8.105E-007	0.13	0.7304	
CD	1.721E-004	1	1.721E-004	26.83	0.0006	significant
Residual	5.773E-005	9	6.414E-006			
Lack of Fit	4.136E-005	6	6.893E-006	1.26	0.4587	not significant
Pure Error	1.637E-005	3	5.458E-006			
Cor Total	0.023	19				

4. 1.3. Effect of Operating Parameters on Temperature

Figure 4.3 in the form of RS's (response surface) shows the effect of significant parameters upon the temperature. As can be seen from the RS's, for either of PVC and PE materials, there is an increase in the value of $\Delta t/mp$ as the parameters such as r/t_o , r/p and ω/f increase. However, the rise in $\Delta t/mp$ with increase in the aforesaid parameters is higher for PE than for PVC. The said rise in temperature can be attributed to increase in tool/sheet contact area due to increase in r/p and r/t and increased rotational speeds relative to feed [31]. This rise in temperature may lead to increased material softening and hence will affect the formability, to be discussed later in the coming section.

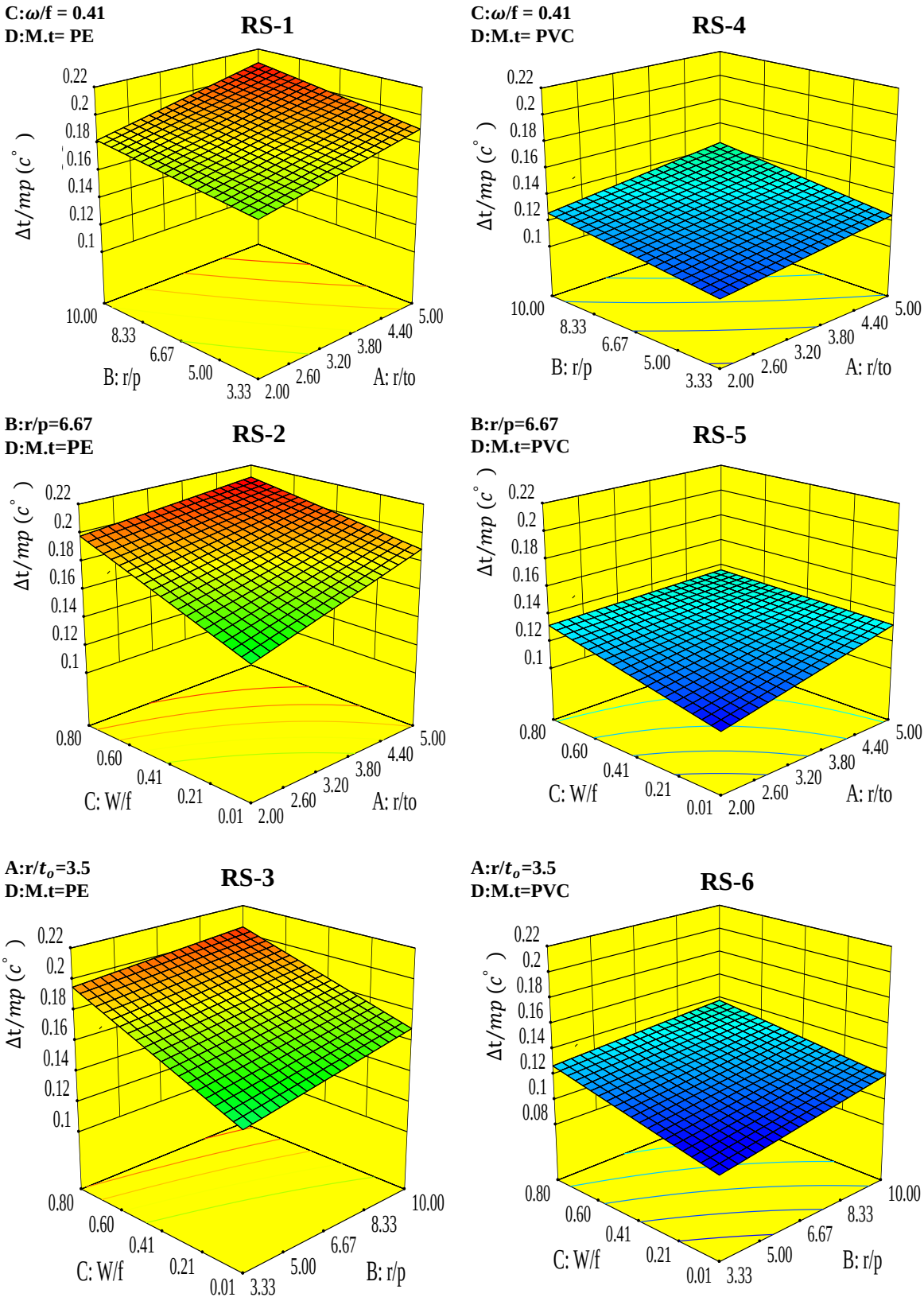

Figure4. 2: Effect of significant liner's on Δt⁄mp (PE and PVC)

4. 1.4.Empirical Formula

The RS's shown in Figure 4.2 graphically illustrate the influence of various parameters on temperature. With the purpose of predicting the effect of parameters on $\Delta t/mp$; regression analysis proposes the following empirical formula.

PE ($\Delta T/mp$) = (4.2)

+0.10977+0.010908* r/t_o+2.62032E-003* r/p +0.092077* ω/f

+2.12394E−004* r/t_o* r/p −0.010066* r/t_o* ω/f −2.11505E-003* r/p * ω/f

PVC($\Delta T/mp$) = (4.3)

+0.066594+8.06355E−003* r/t_o+2.79163E−003* r/p +0.069371* ω/f

+2.12394E−004* r/t_o* r/p -0.010066* r/t_o* ω/f −2.11505E-003* r/p * ω/f

To test the effectiveness of an empirical model two tests are commonly used: The examination of R^2 values (multiple correlation factor) and normal distribution of the residuals [50]. The value of R^2 for the above modle is 99.74%, the predicted R^2 is 98.38% and the adjusted R^2 is 99.46%. The predicted and adjusted R^2 values are in reasenable agreement. So, this test reveals that the datum points are well fitted to the model .

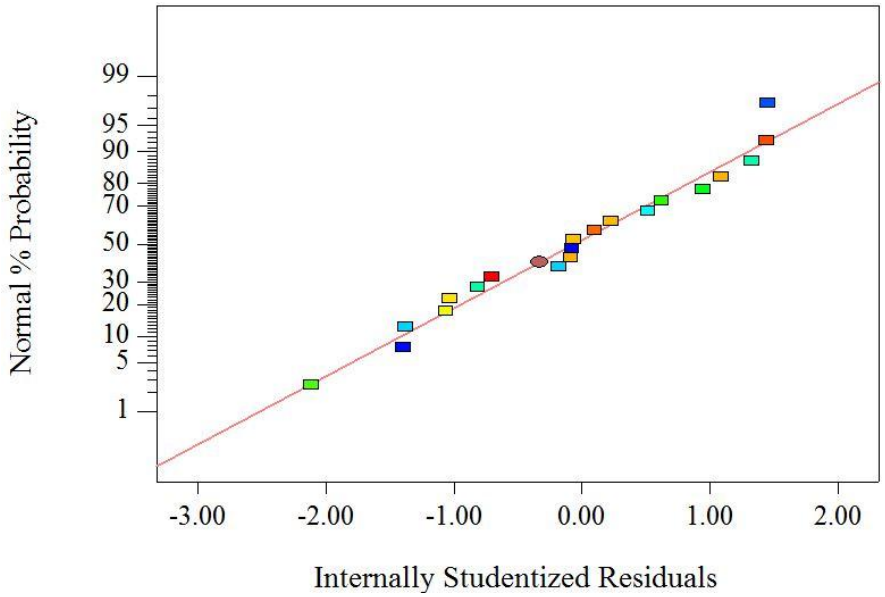

Figure4. 3: Normal plot of residuals (ΔT/mp)

Figures 4.3 is a plot between internally studentized residuals and normal probability. As can be seen from the figure that the residuls properly follow the normal distribution. Since the model reveals high performance in both of the validity tests, it can be stated that the model is correct and therefore is useful for effectively navigating the design space.

4.1. Formability at Fracture

As mentioned in chapter 3, the formability in SPIF (also termed as spif-ability) is often defined as the maximum wall angle [26] that a material withstands without fracturing (θ_{max-f}). This formability measure can be calculated using equation (3.5) given in chapter 3 and as derived in [11].

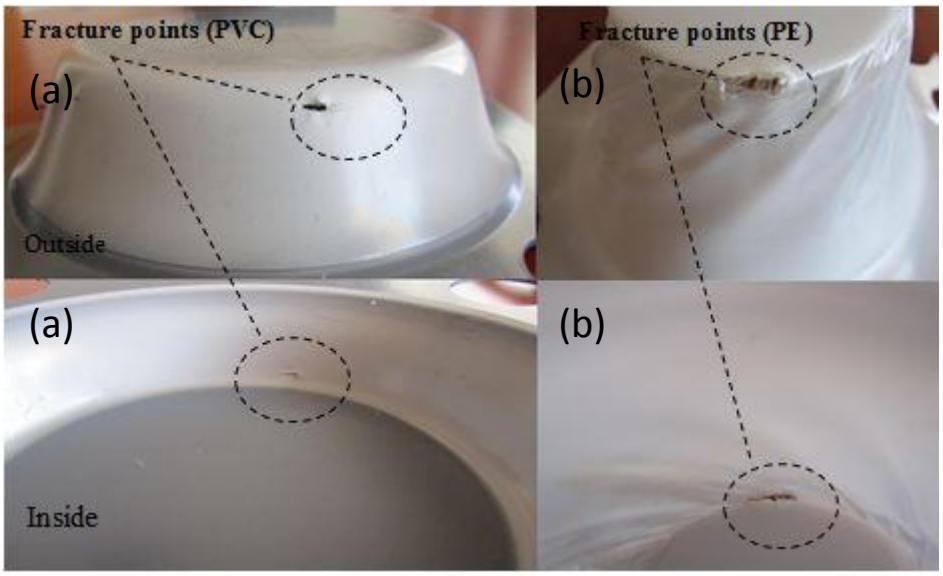

Figure4. 4: Illustration of fracture points on PVC (a) and PE (b) part

4.2.1 Regression Analysis: Significant Parameters for Formability at Fracture

Figure 4.5 represents the results obtained from 20 tests. The maximum and minimum values are belonging to PE (90°)and PVC (62.11°), respectively. To identify the significant parameters and their effect upon the spifability, regression analysis on tests' results was performed with the help of the Design Expert [38].

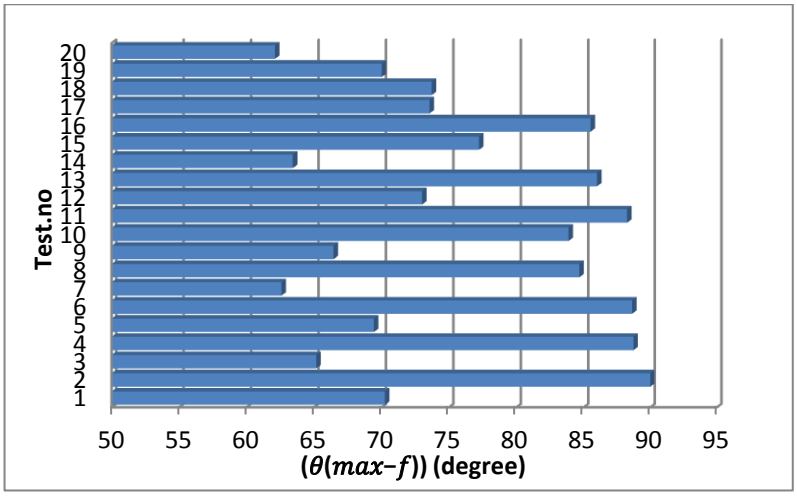

Figure4. 5: The results for (θ_ (max-f))

In the first step, a two-factor interaction (2FI) fit model was opted. Table 4.3 presents the summary of an ANOVA (analysis of variance) of the response surface

2FI model. Again, as was done for temperature, a term with P-value ≤ 5% was considered significant [30]. It is obvious that the model is significant. Moreover, two parameters such as *r/p*, ω/f and categorical parameter D (type of material) significantly influence the θ_{max-f}. In addition, as can be noticed from the table, the interactions between r/t_o& *r/p*, r/t_o& ω/f, r/t_o&*D*, and ω/f &*D* are significant as well. The order of significance of these parameters is given below:

$r/p \geq D \geq r/t_o\, r/p \geq r/t_o\, \omega/f \geq r/t_o D \geq \omega/f \geq \omega/f\, D$

As can be seen from order of significance, the parameters *r/p* and *D* in addition to interactions between r/t_o& *r/p* and r/t_o& ω/f are more significant in contrast with the interactions of r/t_o& *D* and ω/f & *D*.

Table4. 2: ANOVA for Response Surface 2FI Model (θ_ (max-f))

Source	Sum of Squares	df	Mean Square	F Value	p-value Prob > F	significance
Model	1848.60	10	184.86	86.38	< 0.0001	significant
A: r/t_o	6.25	1	6.25	2.92	0.1217	
B: r/p	161.99	1	161.99	75.69	< 0.0001	significant
C: ω/f	19.71	1	19.71	9.21	0.0141	significant
D:M.t	1034.05	1	1034.05	483.18	< 0.0001	significant
AB	84.73	1	84.73	39.59	0.0001	significant
AC	48.97	1	48.97	22.88	0.0010	significant
AD	45.54	1	45.54	21.28	0.0013	significant
BC	0.047	1	0.047	0.022	0.8855	
BD	5.04	1	5.04	2.36	0.1592	
CD	19.10	1	19.10	8.92	0.0153	significant
Residual	19.26	9	2.14			
Lack of Fit	15.47	6	2.58	2.04	0.2982	not significant
Pure Error	3.79	3	1.26			
Cor Total	1867.86	19				

4.2.2 Effect of Process Parameters on Formability Corresponding to Fracture

Figure 4.6 portrays the effect of parameters on the formability at fracture (θ_{max-f}). It can be observed from the RS's 1, 2, 4 and 5 that the combination of low r/p (3.33) and high r/t_o (5), the combination of low ω/f (0.01) and high r/t_o (5) and the

combination of high ω/f (0.8) and low r/t_o (2.00) yields low formability. On the other hand, in all of the RS's, the combination of high r/p (10) and high r/t_o (5), the combination of high ω/f (0.8) and high r/t_o (5) leads to high formability. From these results, it follows that in order to achieve high θ_{max-f} for either of PE and PVC materials, the combinations of high values of parameters (high-high) should be opted: other combinations (such as low-low and low-high) are not very useful. These formability results are in accordance with those discussed above for temperature rise (Figure 4.2). This means at high-high combination of parameters high formability is achieved because large temperature rise ($\Delta t/mp$) occurs which in turn causes softening of material and hence improves formability.

This is to be noticed from Figure 4.3 that PE yields high formability [31], at any combination of parameters, than PVC material. This is due to the fact that the former has high elongation (97.72%) than the latter one (29.22%). Further the effect of variation in parameters (especially high-high combination) on PE is larger than that on PVC. This could be due to higher rise in temperate in PE than in PVC as evidenced in Figure 4.2.

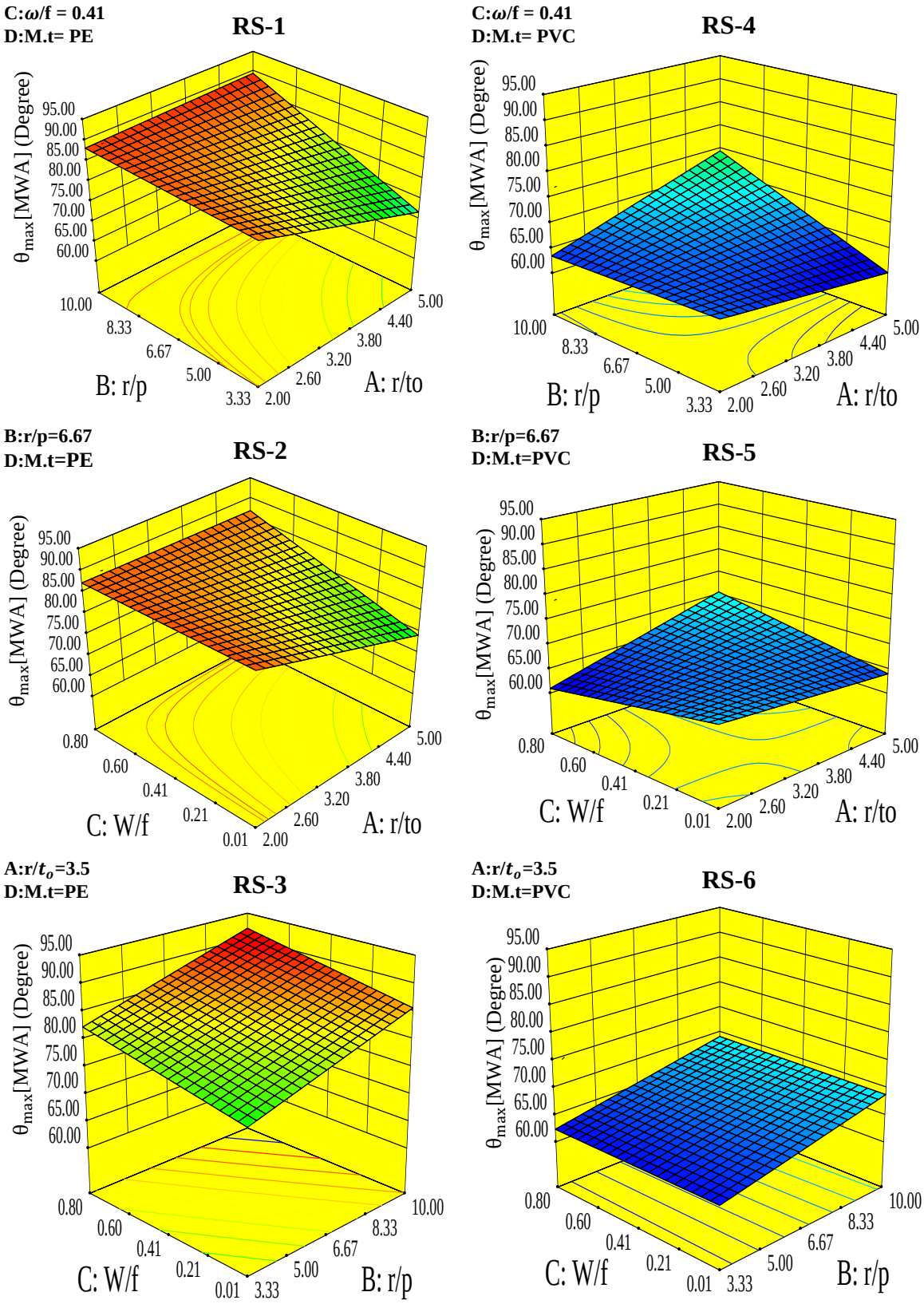

Figure4. 6: Effect of significant 2FI's on Maximum wall angle (PE and PVC)

4.2.3 Empirical Formulae: Formability at Fracture

The RS's shown in Figure 4.6 graphically illustrate the influence of various parameters on formability of PVC and PE sheets at fracture. And can provide guidelines to increase spifability. To predict the formability at fracture for any combination of parameters (but in investigated range), regression analysis proposes the following empirical formulas [45].

PE (θ_{max-f}) = (4.4)

$+105.97831-9.77076 * r/t_o -1.39515 * r/p -11.96116 * \omega/f +0.79677 * r/t_o * r/p +5.47610* r/t_o * \omega/f +0.076323* r/p * \omega/f$

PVC (θ_{max-f}) = (4.5)

$+81.88269-6.46028 * r/t_o -1.82234 * r/p -19.52583 * \omega/f$

$+0.79677* r/t_o * r/p +5.47610*$ r/to $* \omega/f +0.076323* r/p * \omega/f$

The R-squared value (multiple correlation factor) for the model (Eq. 4.4 and 4.5) is 98.9%, the predicted R^2 is 91.4% and the adjusted R^2 is 97.8%. , which means the model well fits to the datum points. In order to further verify the robustness of above proposed model, the normal distribution of residuals (another criterion for testing soundness of an empirical model) is examined in Figure 4.7. As can be seen from the figure, the residuals follow normal distribution. Based on the results of these two tests, it can be said that the model is accurate can be used to navigate the design space. Therefore, the above model can be employed to predict maximum formabilty corrospanding to fracture (θ_{max-f}).

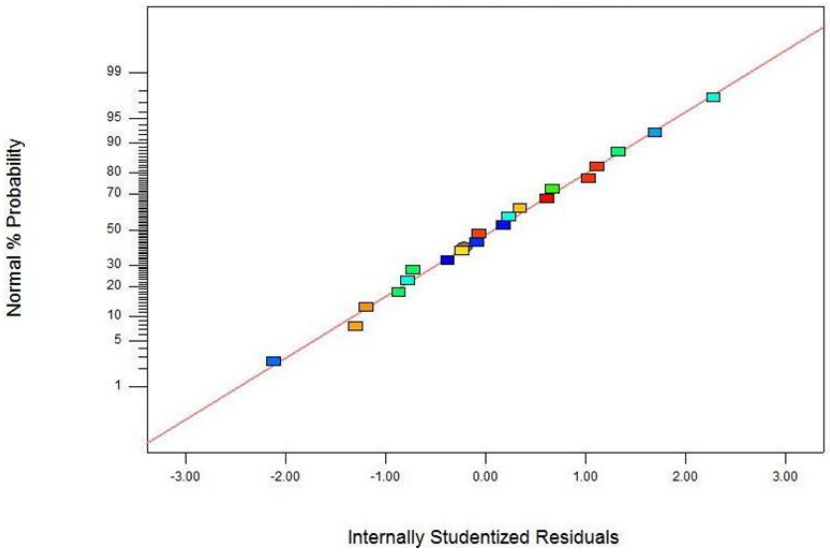

Figure4. 7: Normal Plot of Residuals (formability at fracture)

4.2.4 Optimization: Formability at Fracture

In order to maximize the formability, the derringer-suich multi-criteria decision-making algorithm was applied to the experimental results [45]. Keeping in view the mentioned trend and the factors affecting the spifability ,the optimization criteria was set as following: r/t_o = in range , r/p = in range , ω/f = in range , and θ_{max-f} = maximize.The Design Expert software recommended the following optimal solutions as illustrate in table 4.4.

Table4. 3: Recommended optimal solution by Design Expert software for (θ_(max-f))

Material type	r/t_o	r/p	ω/f	θ_{max-f} (degree)
PE	3.40	9.84	0.69	90.80
PVC	5.00	10.00	0.80	78.09

4. 3. Formability at Wrinkling

As known, the maximum wall angle corresponding to fracture is defined as formability in SPIF. However, this definition is valid for sheet metals and for high strength polymers [26]. In this work, it was found that PE (low strength) wrinkles before fracturing [23]. As was observed during tests, the wrinkles are outcome of material twisting about the axis of revolution in the direction of rotation of the forming tool and are triggered in the region of the inclined wall placed in immediate vicinity of the corner radius, where thinning is more pronounced. During tests, it was found that thinner sheets are more sensitive to wrinkling than thicker ones (see Figure 4.8 for evidence) [29]. Wrinkling is a sign of failure although not fracture. Therefore, for PE it is more appropriate to limit formability corresponding to an angle at which wrinkling begins. Therefore, during tests, maximum value of wall angle corresponding to wrinkling (θ_{max-w}) was recorded for PE; whose regression analysis is presented in the next sub-section. The reader may note down that no wrinkling was observed in PVC: it might be because of the fact that PVC has higher strength (15.125 MPa) than that (5.0125) of PE.

Figure4. 8: Wrinkling phenomenon for three different thicknesses of polyethylene sheets

4.3.1 Regression Analysis: Formability at Wrinkling

Figure 4.9 illustrate the results of θ_{max-w} obtained from 12 tests of PE sheet in SPIF process. The maximum and minimum value respectively belongs to test 4 (77.864°) and test 2 (69.512°).

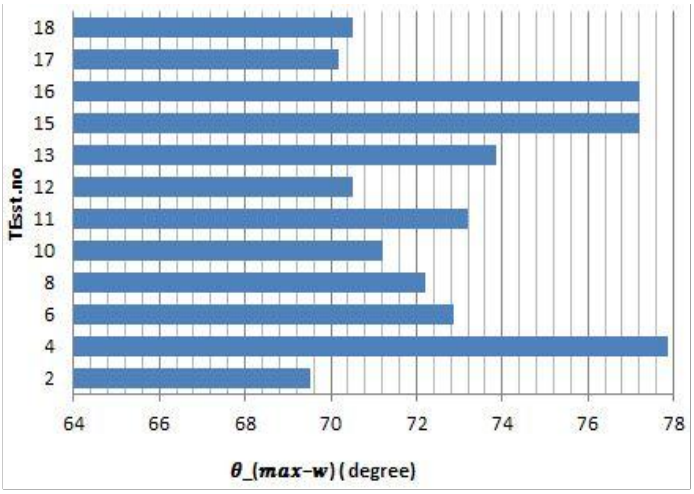

Figure4. 9: Test Results for (θ_(max-w))

To identify the significant parameters and their influence upon the spifability, regression analysis on tests' results was done with the help of the Design Expert software [50]. In the first step, a 2FI model was opted. Table 4.5 presents the summary of an ANOVA of the model. It is clear that the model is significant. Additionally, the parameters such as r/t_o, ω/f and r/p are significant. The order of significance of parameters can be seen as follows:

D > r/p > ω/f > r/t_o > $r/t_o D$ > r/t_o ω/f

Table4. 4: ANOVA for response surface 2FI model (θ_(max-w))

Source	Sum of Square	df	Mean Square	F Value	p-value Prob > F	significancy
Model	294.34	10	29.43	28.30	< 0.0001	significant
A:r/t_o	7.97	1	7.97	7.66	0.0218	significant
B:r/p	28.52	1	28.52	27.42	0.0005	significant
C:ω/f	23.29	1	23.29	22.40	0.0011	significant
D: m.t	119.44	1	119.44	114.85	< 0.0001	significant
AB	0.19	1	0.19	0.18	0.6789	
AC	3.38	1	3.38	3.25	0.1050	significant
AD	24.97	1	24.97	24.01	0.0008	significant
BC	2.56	1	2.56	2.46	0.1512	
BD	0.51	1	0.51	0.49	0.5026	
BC	0.14	1	0.14	0.13	0.7251	
Residual	9.36	9	1.04			
Lack of Fit	8.30	6	1.38	3.90	0.1455	not significant
Pure Error	1.06	3	0.35			
Cor Total	303.70	19				

4.3.2 Effect of Process Parameters on Formability at Wrinkling

Figure 4.10, as response surface (RS), shows the relationship between θ_{max-w} and the various parameters. The examination of RS's shows that by increasing the parameters such as$r/t_o, r/p,\ \omega/f$ the value of θ_{max-w} decreases. Recalling the effect of these parameters on temperature rise (temperature rise increases as the said parameters increase), the said result can be due to increased material softening due to increase in temperature rise. Obviously, increased softening will lead to decrease in strength and hence increased wrinkling and thus causing wrinkling at low angles. These results highlight that to reduce wrinkling or to increase θ_{max-w} , one should choose low values of parameters, contrary toθ_{max-f}.

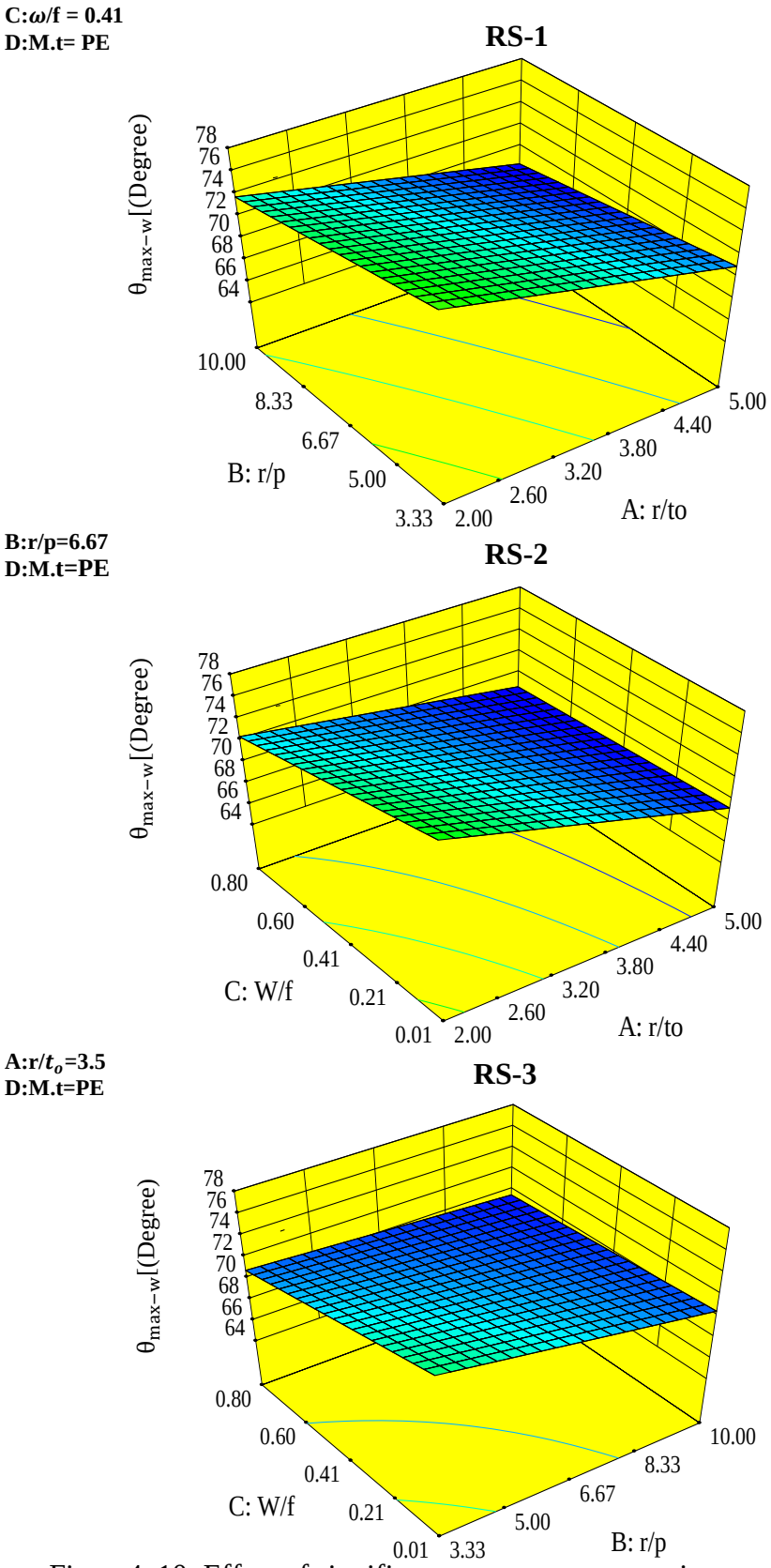

Figure4. 10: Effect of significant parameters on maximum wall angle at wrinkling

4.3.3 Empirical Formula: Formability at Wrinkling

Finally, the regression analysis proposes the following empirical formula:

$$PE(\theta_{max-w}) = \quad (4.6)$$

$$+88.14859-2.72275^{*}\, r/t_o - 0.80057 * r/p - 12.74030^{*}\, \omega/f + 0.037753 * r/t_o * r/p + 1.43799^{*}\, r/t_o * \omega/f + 0.56323^{*}\, r/p * \omega/f$$

The examination of multiple correlation factor (R^2) and normal distribution of the residuals were carried out to test the fitness of an empirical model. The R^2 value for the above model is 96.92%, the adjusted and predicted R^2 are 93.49% and 85.52% in sequence. So, the predicted and adjusted R^2 are in good agreement offers that the datum fairly follows normal distribution [30]. The plot of normal probability against residuals is illustrated in figure 4.7. As can be found the residuals fairly follow normal distribution. Therefore, since the model shows well performance in both of the tests, it can be said that the model is correct and hence can be employed to predict θ_{max-w} in the investigated range of parameters.

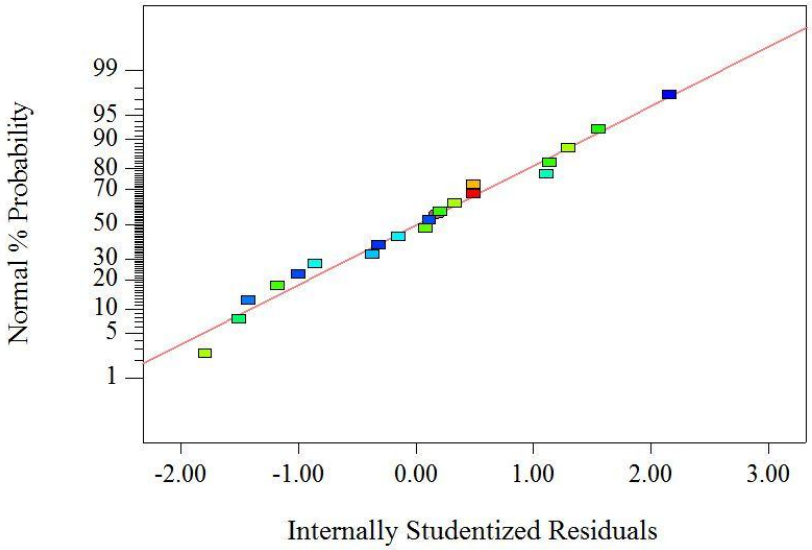

Figure4. 11: Normal plot of residuals (formability at wrinkling)

4.3.4 Optimization: Formability at Wrinkling

To achieve maximumθ_{max-w}, the process optimization can be carried out as follows: ω/f = in range, r/t_o= in range, r/p = in range, and θ_{max-w} =maximized. The Design expert software suggested the following optimal solution: r/t_o= 2, r/p =3.33, ω/f = 0.01. This combination of parameters is believed to provides $\theta_{\max-w}$= 80.2084 °.

In Summary, the above discussed results show that type of material is an important factor, in addition to others, that determines whether wrinkling will occur or not. The properties of polymers (PVC and PE) especially melting point and strength play a major role in this regard. It has been found that a polymer with low melting point and low strength (i.e., PE) is more vulnerable to wrinkling. Also, large high-high combination of parameters leads to reduction in $\theta_{\max-w}$. On the contrary; the same interestingly causes increase in $\theta_{\max-f}$ of both PE and PVC, which has been found to be an outcome of rise in temperature with increase in parameters. Based on the results, it can be said that high-high combinations should be opted for improving $\theta_{\max-f}$ of PVC, whereas low-low combinations should be chosen for improving $\theta_{\max-w}$ of PE.

Chapter 5

CONCLUSIONS AND FUTURE WORK

1. In the current work, the suitability of SPIF process, a novel forming method, to process polymer materials (PVC and PE) was investigated. It has been found that the said novel method can be successfully employed to produce engineered parts, and thus this process can replace costly conventional methods such as injection molding and thermoforming.

2. The results have shown that the formability in PVC is limited by fracture while the formability in PE is limited by wrinkling. Therefore, the formability measure in these materials should be opted as follows: θ_{max-f} for PVC and θ_{max-w} for PE.

3. A variation in either of the investigated parameters, namely r/t_o , r/p and ω/f, affects temperature rise and formability in SPIF of polymers. The analysis for temperature shows that the high-high combination of parameters (e.g. r/to*=5,* r/p*=10,* ω/f*= 0.8*) causes rise in temperature, for both of PVC and PE materials, which in turn poses positive effect on formability at fracture θ_{max-f}. However, this rise in temperature proved detrimental for PE material in the sense that it increases wrinkling. Therefore, to improve the formability of PVC, one should choose high values of the above said parameters. Whereas, in order to improve the formability of PE, low values of process parameters (e.g. r/to *=2,* r/p*=3.33.* ω/f = 0.01) should

be opted so that temperature could be kept as low as possible to prevent softening of material.

4. The empirical models have been proposed in the present work. These models, within the investigated range of parameters, can be used to predict formability for a given set of parameters. Moreover, these are useful for process optimization to achieve high formability in PVC and PE.

5. This study has laid down a direction following which SPIF of further polymer materials of interest can be investigated.

6. During tests, it was observed that wrinkling is reduced as the thickness of a polymer sheet increases. The mechanism and causes of this finding need to be researched in detail, which is proposed as a future work.

REFRENCES

[1] Satyandrak, Gupta. (2002).Sheet metal bending: forming part families for generating shared press-bruke setups. *Journal of manufacturing systems*.21 (5), 329-350.

[2] Jeswiet, E., & Hagan, J. (2003). A review of conventional and modern single point sheet Metal forming methods. *Journal of engineering manufacture*.217, 213–225.

[3] Bewlay, B.P., & Furrer, D.U. (2006).Spinning. ASM Hand book, metalworking, Sheet forming.

[4] Emmens, W.C., & sebastiani, G. (2010). The technology of Incremental sheet Forming: a brief review of the history. *Journal of materials processing technology*210, 981-997.

[5] Wong, c., Dean, T.A., & Jlin. (2003). A review of spinning, shear forming and flow Forming processes. Mechanical and Manufacturing Engineering, School of Engineering, University of Birmingham.

[6] Roy, M.J., Klassenb, R.J., & Woodb, J.T. (2009). Evolution of plastic strain during a flow forming process. *Journal of Materials Processing Technology*. 209, 1018–1025.

[7] Kwiatkowski, L., Sebastiani, G., Shankar, R., Tekkaya. (2008). Towards Full Kinematic Incremental Forming, in Esaform Lyon.

[8] Quigley, Emanon, & Monaghan, John. (2000). Metal forming: an analysis of spinning processes. *Journal of Materials Processing Technology*. 103, 114 -119.

[9] Kalpakcioglu, S. (2007). A study of shear-spinnability of metals, Transactions of the ASME. *Journal of Engineering for Industry.* 83, 478–483.

[10] Altan, Taylan, & Tekkaya, A. Erman (2012).Sheet Metal Forming: Processes and Applications.

[11] Micari, F., Ambrogio, G., & Filice, L. (2007). Shape and dimensional accuracy in Single Point Incremental Forming: State of the art and future trends. *Journal of Materials Processing Technology*. 191, 390-395.

[12] Nakajima, N. (1979). Numerical control for traditional manual forming of sheet metal. *Journal of the Japan Society for Technology of Plasticity*. 23, 696–700.

[13] Martins, P.A.F., Bay, N., Skjoedt, M., & Silva M.B. (2008). Theory of single point incremental forming. *Manufacturing Technology.* 57, 247–252.

[14] Park, J. J., & Kim, Y. H. (2003). Fundamental studies on the incremental sheet metal forming technique. *Journal of Materials Processing Technology*.140, 447-53.

[15] Jackson, Kathryn, & Allwood, Julian. (2009). The mechanics of incremental sheet forming. *Journal of materials processing technology*. 2 0 9, 1158–1174

.

[16] Schaeffer, Lírio. (2009). Development of customized products through the use of incremental sheet forming for medical orthopedic applications. *Conference of Integrity, Reliability and Failure.* 209,308.

[17] Ambrogio, G., & Filic, L. (2007). Shape and dimensional accuracy in single point incremental forming: state of the art and future trends. *Journal of Materials Processing Technology*.191, 390-395.

[18] Jeswiet, J., Micari, F., Hirt, G., Bramley, A., Duflou, J., Allwood, J. (2005). Asymmetric Single Point Incremental Forming of Sheet Metal. *manufacturing Technology*. 54, 88-114.

[19] Ambrogio, G., Filice, L., & Gagliardi, F. (2012). Formability of lightweight alloys by hot incremental sheet forming. *Jornal of Materials & Design* .34, 501–508.

[20] Durante, M., Formisanom, A., Langella, A., & Memola Capece Minutolo, F. (2009) The influence of tool rotation on an incremental forming process. *Journal of Materials Processing Technology.* 209, 4621-4626.

.

[21] Ji, Y.H., & Park, J.J. (2008). Formability of magnesium AZ31 sheet in the Incremental forming at warm temperature. *Journal of Materials Processing Technology*. 201, 354–358.

[22] Gordon, M. J. (2003). Industrial design of plastics products. Wiley-Interscience Publication.

[23] Martin, P.A.F., Kwiatkowski, L., Franzen, V. & Tekkaya A.E. (2009).Single point incremental forming of polymers. *Manufacturing Technology*. 58,229–232.

[24] Malhotra, Rajiv, Xue, Liang, Belytschko, Ted, & Cao, Jian. (2012). Mechanics of fracture in single point incremental forming. *Journal of Materials Processing Technology*. 212, 1573– 1590.

[25] Jacksona, K.P., Allwooda, J.M., & Landertb, M. (2008). Incremental forming of sandwich panels. *Journal of materials processing technology*.2 0 4, 290–303

[26] Hussain, G., & Gao, L. (2007).A novel method to test the thinning limits of sheet metals in negative incremental forming. *International Journal of Machine Tools& Manufacture*. 47, 419–435.

[27] Hamilton, K., & Jeswiet, J. (2010). Single point incremental forming at high feed rates and rotational speeds: Surface and structural consequences. *Manufacturing Technology*. 59, 311–314.

[28] Franzen, V., Kwiatkowski, L., Martins, P.A.F.,&Tekkaya, A.E. (2008).Single

Point incremental forming of PVC. *Journal of Materials Processing Technology*.209, 462–469.

[29] Silva, M.B., Alves, L.M., & Martins, P.A.F. (2010). Single point incremental forming of PVC: Experimental findings and theoretical interpretation. *European Journal of Mechanics*. 29, 557–566.

[30] Hussain, G., Gao, L., Hayat, N. (2011). Forming parameters and forming defects in incremental forming of an aluminum sheet. Correlation, empirical modeling and optimization. *Materials and Manufacturing Processes*. 26, 1546–1553.

[31] Tania, A., Marques, Silva, Maria Beatriz, & Martins, P. A. F. (2012). On the potential of single point incremental forming of sheet Polymer parts.

[32] Baeurle, S.A., Hotta, A., & Gusev, A.A. (2006). On the glassy state of multiphase and pure polymer materials.

[33] Ziabicki, A. (1976). Fundamentals of fiber formation, John Wiley and Sons, London.

[34] Rosado, D. (2000). Injection Molding Handbook. Kluwer Academic Publishers.

[35] Lee, N. (2008). Blow Molding Design Guide (2nd ed.), Hanser -Gardner Publications.

[36] Tanaka, T., Conrad, H. (2004). Deformation kinetics for slip in titanium single

crystals below 0.4Tm. Metallurgical Engineering and Materials Science Department. University of Kentucky Lexington.

[37] Yin, K.F., Wu, D.L., Zhang, D.Z. (2006). Formability of AZ31 magnesium alloy sheets at warm working conditions. *International Journal of Machine Tools and Manufacture.* 46, 1276-1280.

[39] Arnold, P. (2008).Incremental Sheet Forming with a Robot System for an Industrial Application. Manufacturing Systems and Technologies for the New Frontier.

[40] Hirt, G., Ames, J., Bambach, M., Kopp, R. Forming Strategies and Process Modeling for CNC incremental Sheet Forming. *Annals of CIRP*. 53, 203.

[41] Junk, S., Hirt, G. I. (2003). Chouvalova. Forming Strategies and Tools in Incremental Sheet Forming. *Proceedings of the 10th International Conference on Sheet Metal*. 57-64.

[42] Jeswiet, J., & Nyahumwa, C. (1993). A sensor for measuring metal deformation interface forces. *Journal of Materials Processing Technology*. 39, 251–268.

[43] Duflou, J., Szekeres, Van Herck, A. (2005). Force Measurements for Single Point Incremental Forming: and experimental study. *Journal Advanced Materials Research*. 441-44.

[44] Jeswiet, J., & Young, D. (2004). Wall thickness variations in single-point Incremental forming .Proceedings of the Institution of Mechanical Engineers,

Part B: *Journal of Engineering Manufacture*. 218, 1453-1459.

[45] Hussain, G., Gao1, L. (2009). Empirical modeling of the influence of operating Parameters on the spifability of a titanium sheet using response surface methodology. *Journal of Engineering Manufacture*. 223- 73.

[46] Micari, F., Filice, L., & Fratini, L. (2002). Analysis of Material Formability in Incremental Forming. *CIRP Annals - Manufacturing Technology*. 51, 199–202.

[47] Wei, H.Y., Gao, L., & Li, S.G. (2004). Investigation on thickness distribution along bulge type incrementally formed sheet metal part with irregular shapes. *International Manufacturing Conference*. 1672–3961.

[48] You-Min, Huang., Yuung-Hwa, Lua. (1992). Elastic-plastic finite-element analysis of V-shape sheet bending. *Journal of Materials Processing Technology*. 35,129-150.

[49] Oyane, M., &T Sato. (1980) .Criteria for ductile fracture and their applications Journal of Mechanical engineering. *Work Tech*. 4, 65–81.

[50] Pohlak, M. (2004) .Modeling and optimal design of the incremental forming process.*Proc.Estonian Acad.Sci. Eng.* 10, 261-269.

[51] Iseki, H.(2001). An approximate deformation, analysis and FEM analysis for the incremental bulging of sheet metal using a spherical roller. *Journal of Mater*

Process Technol. 111,150–154.

[52] Eyckens, P., Van Bael, A., Duflou, J. R., Aerens, R. (2009). Force prediction for single point incremental forming deduced from experimental and FEM observations. 10.1007/s00170-009-2160-2.1433-3015.

Appendix A: Stress-Strain Curve (PVC&PE)

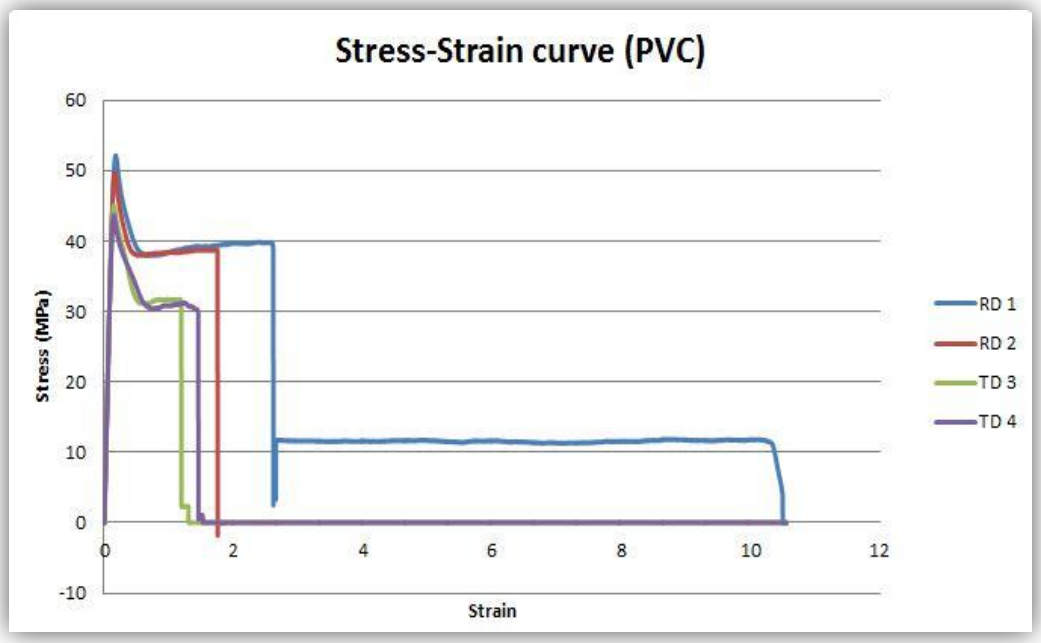

Stress strain curve (PVC)

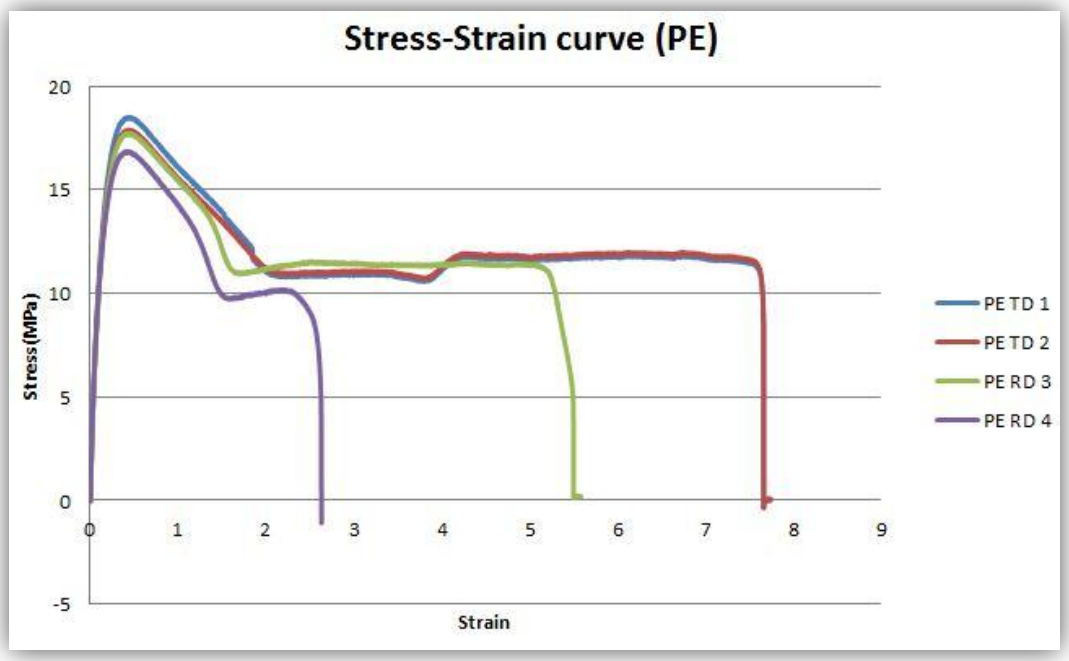

Stress-strain curve (PE)